CLIMATE CHANGE IMPLICATIONS TO IRRIGATED RICE PRODUCTION IN
SOUTHERN BRAZIL: A MODELLING APPROACH

A DISSERTATION
SUBMITTED TO THE FACULTY OF THE
UNIVERSITY OF MINNESOTA
BY

THIAGO DOS SANTOS

IN PARTIAL FULFILLMENT OF THE REQUIREMENTS
FOR THE DEGREE OF
DOCTOR OF PHILOSOPHY

TRACY E. TWINE

AUGUST 2017

Dedication

I dedicate this dissertation to my parents, Iracema Veloso and José Aparecido (*in memoriam*), my friends and loved ones.

Abstract

Rice is one of the staple foods for more than three billion people worldwide.
When cultivated under irrigated conditions (i.e. lowland rice), rice is one of the most
intensive water consumer crops globally. Therefore, representation of rice growth should
be integrated into the latest land surface models to allow studies on food security and to
ensure that accurate simulations of the bidirectional feedbacks between the land surface
and atmosphere take place. In this study, I present a new process-based model for rice
fields that includes rice growth and rice irrigation as modules within the Agro-IBIS
dynamic agro-ecosystem model. The model includes a series of equations, agricultural
management parameters and an irrigation scheme that are specifically tailored for rice
crops. The model was evaluated against leaf area index and biomass observations,
obtained for one growing season in Rio Grande do Sul state (southern Brazil), and in Los
Baños, Philippines. The model accurately captured the temporal dynamics of leaf area
index in both the Brazilian and the Philippine sites, and predicted end-of-season biomass
with an error of between -9.5% and 11.3% depending on the location and the plant organ.
Rice phenology is predicted by the model based on experimentally-derived growth rates,
and was evaluated by comparing simulated and observed durations of the four growth
phases considered by the model. Agro-IBIS showed a tendency to overestimate the
duration of the growth stages between 3% and 16%, but underestimated by 8% the
duration of the panicle formation phase in one growing season. The new irrigation model
is based on the water balance at the surface and applies irrigation in order to keep the
water layer at the paddy field always in the optimum level.

A set of climate projections from global climate models under two emission scenarios, and excluding and considering CO_2 fertilizations effects, was used to drive the updated Agro-IBIS to estimate the effects of climate change on rice phenology, productivity and irrigation demand in southern Brazil during the 21st century. The results suggest that rice yields in southern Brazil can increase in average by 10–30%, but by up to 80% in regions where the current temperature is below optimum for rice growth and therefore will be benefited by warming. However, the same region might experience higher water demand for rice irrigation, which might pose a challenge for rice production in that region.

Table of Contents

List of Tables

List of Figures

Chapter 1. Introduction

Rice (*Oryza sativa*) is one of the world's most important cereal food crops, mainly in Asia but increasingly so in Africa and Latin America. Rice provides a significant portion of the dietary requirements to nearly 2.6 billion people, including another 400 million people relying on rice for quarter to half of their diet (McLean, Hardy, & Hettel, 2013). Thus, for many countries, national self-sufficiency in rice production is a crucial matter. Rice is grown from as far north as Manchuria in China and California in the US to as far south as New South Wales in Australia and central Argentina (Khush, 2005). Figure 1 shows the global distribution of rice production for the year 2014.

Rice can be cultivated either as an upland (aerobic) or wetland (irrigated or rainfed) crop. It is estimated that upland rice cultivation covers 17 million hectares, while wetland rice is cultivated on 131 million hectares, contributing to about 30% and 70%, respectively, of the total rice production in the world (FAO, 2016). When cultivated irrigated, rice is considered one the most water-demanding crops globally because a standing water layer needs to be established in the fields during soil preparation and maintained throughout the growing season (Bouman, Humphreys, Tuong, & Barker, 2007).
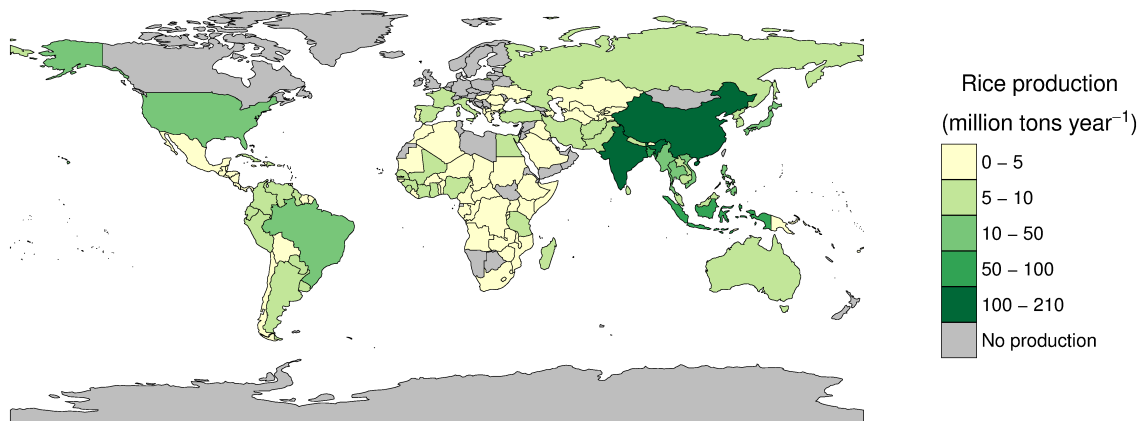
Figure 1. Global paddy rice production in 2014 (based on data from FAO, 2016)

It is estimated that global rice production levels seen in 1990 will need to increase by at least 46% by the year 2050 in order to keep up with a rapidly increasing world population (Alexandratos & Bruinsma, 2012). Potential future climate change resulting from steadily-rising atmospheric carbon dioxide (CO_2) concentration and other greenhouse gasses limits the ability to predict global rice production (B. A. Kimball, 1983) and raises serious questions concerning food security for the near future. Hence, accurate projections of the impacts of climate change on rice productivity on a region-by-region basis are essential, not only for the estimation of world food security, but also for the continued sustainability of rice growers, which in most countries consist of subsistence farmers (McLean et al., 2013).

Brazil is the ninth-largest rice-producing country and the largest outside Asia, with a production of 12.2 million metric tons in 2014, or about 1.3% of the world's rice production (Table 1). In southern Brazil, agriculture plays an important economic role and represents the region's main water consumer since irrigated rice is the most important system of production. In 2014, irrigated rice paddies covered 50.9% of the total

area under cultivation and accounted for 78.6% of the production; upland rice occupied

49.1% of the area and produced 21.4% of the total (Brazilian Institute for Geography and

Statistics, 2015).

Table 1. The top ten rice producing countries in the world (Source: FAO 2016)

Rank	Country	% of global production
1	China	21.94
2	India	16.56
3	Indonesia	7.46
4	Bangladesh	5.50
5	Vietnam	4.74
6	Thailand	3.44
7	Myanmar	2.78
8	Philippines	2.00
9	Brazil	1.28
10	Japan	1.11

In southern Brazil, it is estimated that the cost to deliver water to farms represents

about 12-18% of total crop expenses (National Supply Company, 2016). In most

productive regions, it is currently the water availability for rice cultivation, rather than

variations in the temperature, that is a limiting factor for achieving high yields.

Exacerbated withdrawals in the period of greatest water demand by the culture poses the

risk of lowering the level of lakes and reservoirs, bringing consequences for the

environment and insecurity on the part of producers. Assessment of changes in irrigation

requirement under scenarios of climate change is critical to long-range planning for water

resource allocation since agriculture is one of the primary water users in Brazil.

In the last two decades, efforts have been made to better understand regional and

global environmental changes caused by land surface-atmosphere interactions. Examples

of such interactions include activities that change the properties of the land surface and

can cause significant effects on the climate, such as afforestation and deforestation, urbanization and agricultural practices.

For example, according to Ramankutty et al. (2008) in the year 2000 croplands covered about 15.1 million km^2, while pasture covered approximately 28.3 million km^2, representing a combined total of about 30% of the global land surface. This significant area of agricultural land is likely to considerably increase in the next decades under the pressure of an increasing global population, the associated need for increased food production, and the recent expansion of crop-based biofuels production. These land use changes have the potential to greatly influence biogeochemical and biogeophysical processes across the world.

These changes in the biosphere are usually investigated using Land Surface Models (LSMs), which simulate hydrological and biochemical processes, energy, water and carbon exchanges between the lower atmosphere and land surfaces. LSMs are often coupled to Regional Climate Models (RCMs), which then allows for a more realistic representation of atmospheric transportation of water, heat and momentum that occur at large geographic scales.

Many studies have highlighted the importance of bidirectional interactions between the biosphere and the atmosphere. For example, applying a RCM combined with a crop growth model (CGM) to the United States, Tsvetsinskaya et al. (2001) showed that the resulting changes in surface heat fluxes caused by crop growth can change the surface temperature by 2–4°C. In the Midwestern United States, Georgescu et al. (2011) replaced annual by perennial crops in the Weather Research and Forecasting model (WRF) and estimated a significant cooling effect at the surface as a result of increases in transpiration

and higher albedo caused by that transition. Levis et al. (2012) incorporated a crop growth model into the Community Earth System Model, and showed that the timing of crop sowing can change the amount of precipitation in Midwestern North America. All these studies indicate that crop growth and land use and cover changes are key determinants of climate and that climate simulations need to simulate the fluxes of heat, water, and gases over agricultural land.

Among the latest generation of LSMs, only JULES-crop (Osborne et al., 2015) currently simulates the growth of rice, although rice is one of the major global crops, accounting for approximately 23% of agricultural land farmed with cereals worldwide (FAO, 2016). Even so, JULES-crop does not consider the irrigated and flooded surface of paddy rice fields, which is an important parameter when simulating heat and water fluxes in paddy rice fields, because heat and water fluxes in a flooded and irrigated surface are largely different from those in a non-flooded and rain-fed surface (Biggs et al., 2008; Boucher, Myhre, & Myhre, 2004).

In this dissertation, a new process-based model of rice growth and rice irrigation was integrated into the LSM Agro-IBIS (Kucharik, 2003). The growth sub-model was based on the ORYZA2000 crop model (Bouman et al., 2001), and the irrigation sub-model was based on the FAO guidelines for rice irrigation (Brouwer, Prins, & Heibloem, 1989). The model was parameterized and validated at experimental sites in southern Brazil and in the Philippines. Then, as the first application of the updated model, future climate projections were used to drive Agro-IBIS in order to explore possible impacts of climate changes on rice productivity and water consumption in southern Brazil in the 21st century.

The research presented in this dissertation will result in two research articles. The first one, covering the development of the irrigation scheme and exploring possible changes in water requirements caused by climatic changes, was submitted to the peer reviewed international journal *Climatic Change*. At the time of this writing, it is under review. The research on possible impacts of climate change on rice productivity is under preparation to be submitted to a journal in the environmental science field, such as *Global Change Biology* or *Agricultural and Forest Meteorology*.

This dissertation is organized as follows: chapter 2 describes a comprehensive review of the potential effects of climate change on rice development and irrigation water demand. Chapter 3 describes the steps taken to develop and parameterize the integration of a rice growth and a lowland rice irrigation submodules into the Agro-IBIS model, as well as the preparation of the current and future climate scenarios that were used by Agro-IBIS to run the simulations for the 21st century. Chapter 4 describes the validation of the model against observations in Brazil and in Philippines, as well the responses of rice phenology, productivity and irrigation to the projected climate change the 21st century. Chapter 5 presents the overall conclusions of the work, as well as some recommendations for future studies.

Chapter 2. Review of relevant literature

2.1   Temperature effects on rice development

Crop responses to temperature depend on the specific optimum temperature for

photosynthesis, growth and yield (Baker, Allen, & Boote, 1992). The air temperature

range for vegetative growth of rice is generally from 11 to 40°C, with an optimum

between 25 and 33°C (Yoshida, 1981). A seasonal total of at least 2100 growing degree-

days for a period with a daily mean temperature above 10°C is the climatological

requirement for a typical rice cultivation (Yoshida, 1981). If the temperature is below

optimum for photosynthesis, a slight increase in temperature may lead to increased plant

growth and development. However, if temperature is already at or beyond the crop's

optimum, even small increases in temperature have the potential to adversely affect crop

growth and, as a result, decrease yield (Baker & Allen, 1993). Exposure to higher

temperatures causes faster development in crops, which does not necessarily translate

into maximum production because a shorter life cycle means smaller plants, a shorter

reproductive phase, and reduced yield potential because of reduced cumulative light

interception during the growing season (Jagadish, Craufurd, & Wheeler, 2007).

During the reproductive development, rice is particularly sensitive to low

temperatures. At the boot stage, when pollen grains are in the early microspore phase,

constant temperatures below 15°C may inhibit pollen development (Nishiyama, 1984).

Likewise, temperatures below 20°C at the flowering stage generally result in increases in

spikelet sterility (Matsui, Omasa, & Horie, 1997). Therefore, yield losses due to low

temperatures are a major constraint in rice cultivation in areas at high latitudes or high

altitudes such as in northern Japan and areas with similar climate such as parts of

Australia (Farrell, Fox, Williams, & Fukai, 2006), United States (Board, Peterson, & Ng, 1980), Senegal (Dingkuhn, Sow, Samb, Diack, & Asch, 1995) and Korea, northeastern China, Bangladesh, India, Nepal, and other Asian countries (Kaneda & Beachell, 1974). In Brazil, the rice crop may suffer damage from cold occurrence in Rio Grande do Sul (RS), the southernmost State, where more than 60% of the Brazilian rice grain is produced. In this region, as well as in Uruguay and Argentina, low temperatures have been reported to reduce up to 25% of the final yield in anomalously cold years (Bierlen, Wailes, & Crammer, 1997).

High temperatures also reduce plant biomass, by adversely affecting crop reproductive organs and processes. One of the critical phenological stages for high temperature impacts in rice is the reproductive stage because of the effect on pollen viability, fertilization, and grain or fruit formation (Prasad, Boote, Allen, Sheehy, & Thomas, 2006). Jagadish et al. (2007) reported that high temperatures (35°C) during anthesis (the beginning of flowering) and microsporogenesis (pollen generation) resulted in 71 and 34% decline in the spikelet fertility, respectively. One strategy usually employed by genetically-adapted rice plants to avoid sterility caused by higher temperatures is to advance anthesis towards early hours of the morning when the temperatures are cooler (Prasad et al., 2006). This heat tolerance identification might be crucial to mitigate future climatic changes, as there is evidence (to mention one example) that minimum temperature during the night increased by 1.13°C from 1979–2003 in Philippines.

2.2 Combined effects of elevated CO_2 and temperature

The responses to elevated atmospheric CO_2 have been examined on several crops, both C_3 and C_4 (B. A. Kimball, 1983; B. A. Kimball, Kobayashi, & Bindi, 2002; Bruce A. Kimball, 2016). The current ambient CO_2 concentration is a limiting factor for C_3 plants, and rising atmospheric CO_2 will benefit this group of plants because the ribulose-1,5-bisphosphate carboxylase/oxygenase (Rubisco) enzyme can fix more CO_2 due to increased $CO_2:O_2$ ratio, and that results in reduced photorespiration (Baker & Allen, 1993). Increased biomass production due to enhanced photosynthesis has the potential to increase yield, as long as flowering and grain-filling are not disrupted by environmental stresses such as drought or high temperature (Baker et al., 1992). In rice, increase in grain yield can be associated with the response of various components to elevated CO_2, like tiller number per ground area, increased panicle weight at maturity, seed fill and individual grain weight (Kim, Lieffering, Kobayashi, Okada, & Miura, 2003), but not necessarily all components are always benefited by elevated CO_2.

A question that still remains uncertain in the study of global climate change effects on rice is whether the combined effects of elevated CO_2 and rising temperature (which is likely to happen in a future climate) will result in stimulation or inhibition of photosynthesis, and how they translate to changes in biomass and yield. Here, rather contradictory results have been reported. For example, Nakagawa et al. (1997) and Lin et al. (1997) reported that higher temperatures in Philippines and Japan, respectively, stimulated single-leaf photosynthesis of rice exposed to long-term elevated CO_2 treatments during the vegetative stages. On the other hand, Baker and Allen (1993) found that rice canopy photosynthesis was relatively unaffected by a wide range of air

temperatures in southern United States. Response of rice with respect to biomass and yield under CO_2 and/or temperature studies can vary considerably under field condition and in growth chamber studies (Ziska, Weerakoon, Namuco, & Pamplona, 1996). Studies show much larger stimulation (70%) in growth chambers compared to field experiments (10–30%) (Horie, 1993).

The conflicting results reported in the literature about the interactive effect of elevated CO_2 and temperature seem to arise from at least three sources of uncertainties: different experimental conditions, locations in the globe and cultivars studied. There are usually two kinds of experimental systems that have been used to investigate the impact of elevated temperature and super ambient CO_2 on crop plants. One category consists of controlled systems that continuously monitor and recondition the air in growth chambers. These include closed-chamber systems, open-top chambers and temperature gradient chambers. At the other end are free-air CO_2 enrichment (FACE) systems, where CO_2 is continuously sprayed over an experimental plot which is usually 5–20 meters in diameter.

One disadvantage of closed chamber systems is that they are generally small and can significantly alter canopy microclimate compared with plants grown under outdoor conditions (Bruce A. Kimball, 2016). FACE systems, on the other hand, exert no effects on microclimate and can be applied to fairly large cropping areas (Ainsworth & Long, 2005). However, controlling temperature in a FACE system is a challenge. Moreover, it has also been suggested that the CO_2 concentration in FACE is not steady, but rather fluctuates during periods of air turbulence, and the fluctuating CO_2 concentration produces smaller responses than expected (Bunce, 2013).

There are not many studies reporting the interactive effects of both higher temperature and CO_2 on rice. Recently, a soybean FACE experiment (with CO_2 treatments of 380 and 580 ppm) combined with canopy warming by arrays of infrared heaters showed that warming of 3.5°C above ambient reduced the stimulatory effect of elevated CO_2 on photosynthesis (Ruiz-Vera et al., 2013). In a similar experiment at the Japanese rice FACE facility, Usui et al. (2016) investigated the combined effect of two CO_2 treatments – ambient (330 ppm) and 180 ppm above ambient – and soil and water warming (normal temperature and 2°C above normal) on rice productivity. They found that brown rice yield increased by an average of 13.9% under the elevated CO_2 treatment, but no yield increase was observed in the elevated temperature treatment. Aboveground biomass, however, responded positively to both treatments: a 13.5% increase under the CO_2 treatment but only a 3.5% increase in the temperature treatment. Grain yield was significantly increased by elevated CO_2 across a 3-year FACE experiment in Japan (Kim et al., 2003). In the same experiment, yield enhancement due to elevated CO_2 was 15% at medium and high nitrogen fertilization levels, whereas that at low nitrogen level it was only 7%. This suggests that in order to keep higher yields under an elevated CO_2 environment, more fertilization would have to be used.

Potential photosynthetic acclimation (also referred to as photosynthetic down-regulation) in rice as a response to elevated CO_2 has been studied in a few experiments (Baker, Allen, & Boote, 1990; Baker, Allen, Boote, Jones, & Jones, 1990; Rowland-Bamford, Baker, Allen, & Bowes, 1991; Vu, Allen Jr., & Bowes, 1997). Acclimation, which occurs after prolonged exposure of plants to elevated CO_2, is characterized by a lower leaf photosynthetic capacity which is attributed to lower concentrations of Rubisco

(Rowland-Bamford et al., 1991; Vu et al., 1997). The exact mechanism that causes the reduction in Rubisco concentration is still unclear, but one hypothesis is the accumulation of soluble carbohydrates driven by higher photosynthesis rates (Makino et al., 2000).

Differences in acclimation were found by growing soybean and rice under a range (160-990 ppm) of CO_2 concentrations. Soybean photosynthesis, biomass, and yield increased over the whole growth range up to 990 ppm, whereas with rice the greatest increases occurred below 500 ppm (Vu et al., 1997). Even though both are C_3 plants, enhancement effects in rice saturated well below those of soybean, and below predicted CO_2 values for the 21st century. It is not clear whether CO_2 acclimation is the rule or the exception. While Baker et al. (1990a) found no photosynthetic down-regulation in rice grown under CO_2 ranging from 160 to 1000 ppm, a meta-analysis performed by Ainsworth (2008) revealed that rice yield increases at CO_2 concentrations 600–699ppm compared to ambient ranged from 2–20% in FACE systems to 25–110% in greenhouses.

In this dissertation, I use the updated Agro-IBIS model, driven by bias-corrected climate projections, to examine the impacts of future climate extremes on the southern Brazilian rice production. I Specifically answer two questions: (i) How do future climate extreme temperatures affect the phenology and yield of rice in southern Brazil? (ii) How much can CO_2 fertilization compensate the yield loss caused by temperature extremes?

2.3 Rice and water use

Rice is a unique crop in the sense that it is the only cereal that develops in aquatic (i.e. flooded) conditions. Although rice can also be grown on non-flooded soils, best yields are typically achieved under continuously flooded conditions (Bouman et al.,

2007). The height of the water level in paddy fields exerts a strong influence on the development of rice plants. It affects, among other factors, the volume of water used, and consequently, the cost of irrigation. Besides sustaining the evapotranspiration rates, submergence of rice fields by irrigation helps to control adequate supplies of fertilizers, inhibits the presence of weeds, and contributes to maintaining crop temperature, which is important in places where damages caused by low temperatures can occur (Roel, Mutters, Eckert, & Plant, 2005).

Bouman et al. (2007) reviewed the water usage by rice irrigation over the globe. About 90 percent of the world's rice is produced in irrigated or rainfed lowland fields (paddies). Lowland rice needs to account for land preparation requirements, seepage, percolation, evaporation and transpiration. Combined seepage and percolation, for example, range from one to five mm day^{-1} in heavy clay soils to a considerable 25–30 mm day^{-1} in sandy and sandy-loam soils. Typical evapotranspiration rates of rice in Asia range from four to seven mm day^{-1} (Tuong, Cabangon, & Wopereis, 1996). For a typical 100-day season of modern high-yielding rice, the total water input varies from 700 to 5300 mm, depending on climate, soil characteristics and hydrological conditions (Bouman et al., 2007).

In recent years, several studies have been conducted to quantify the water footprint of various crops. Water footprint is defined as the volume of water which is used to produce a particular good, measured at the point of production (Chapagain & Hoekstra, 2011). The estimated global water footprint related to crop production in the period from 1996 to 2005 was 7,404 billion cubic meters per year. The water footprint for rice production was 992 Gm^3 year^{-1}, which consisted of 13% of the total water footprint

of crop production of the world. The water footprint of rice is larger than that of other crops (Chapagain & Hoekstra, 2011).

Climate change will affect temperature and rainfall patterns (IPCC, 2013), and these will likely impact irrigation water requirements. The capacity of the atmosphere to hold water will increase, potentially leading to more precipitation globally which would in theory reduce water demand by crops. However, not all regions of the world will experience an increase in precipitation. Depending on regional conditions and crop varieties, climate variability may produce either positive or negative effects. In locations where annual evaporative demand considerably exceeds annual precipitation, for example in arid regions, higher air temperatures, along with limited moisture availability, may lead to lower relative humidity in the future than are experienced today and therefore enhance irrigation water demands (Seager et al., 2013).

Various studies on the water requirements of paddy rice with regard to climate change have been performed regionally and globally. Döll (2002) presented the first global analysis of impact of climate change on irrigation water requirement using a newly developed global irrigation model. De Silva et al. (2007) projected an increase of 13-23% in irrigation water requirement (IWR) in Sri Lanka for paddy rice during the wet season (October-February). Using projected changes in temperature and precipitation, Shahid, 2011 projected an increase of 0.8 mm day^{-1} in IWR in dry-season rice field in northwest Bangladesh by the end of the century. Chung et al. (2011) estimated decreases in IWR of 4–10% in South Korea when using HadCM3 outputs for the A2 and B2 scenarios in the 2050s and the 2080s. Konzmann et al. (2013) presented simulated IWR globally for 10 crop functional types using the LPJmL global dynamical vegetation model combined

with the output from 19 different global circulation models, and found changes of about -40 to 40% in IWR over major productive agricultural regions across the world by the 2080s. Rodríguez Díaz et al. (2007) projected a rise in irrigation demand of 15–20% by 2050 in the Guadalquivir river basin in Spain, yet to date there have been no projections of changes in IWR in the rice-growing region of Brazil.

In southern Brazil, temperature is expected to rise by 1.9–3.9°C and precipitation is anticipated to increase by 1–12% by the end of the century as compared to the current climate (Giorgi & Diffenbaugh, 2008; Marengo et al., 2010, 2012). However, to my knowledge, there is no research focusing on the need for irrigation in Brazil under climate change scenarios. In this study, I investigate the role of future climate change on water usage for irrigated rice in southern Brazil up to the year 2100. To achieve this, I combine an improved version of the global dynamic vegetation model Agro-IBIS (Kucharik & Brye, 2003) with two future climate scenarios.

This study represents a new focus area within the body of top rice-producing countries in the world. I focus on irrigation requirements because they can be considered a metric of demand on the hydrological system – a key determinant of both rice production costs and environmental sustainability. I test the hypothesis that projected changes in the climate through the end of the century influences the amount of water required to cultivate rice. In the next section, I present the steps taken to integrate the rice growth and rice irrigation models into Agro-IBIS, as well as the methods employed to estimate rice irrigation demands and rice production in a changing climate within an integrated modelling framework.

Chapter 3. Data and methods

3.1 Study area

The southern region of Brazil, here defined as the area between 22°S and 34°S and 58°W and 48°W, comprises the states of Paraná (PR), Santa Catarina (SC) and Rio Grande do Sul (RS). The region, which is depicted in Figure 2, accounts for about 80% of the national rice production (Brazilian Institute for Geography and Statistics, 2015), from which the state contributions are 1.3% , 8.8% and 70.4%, respectively by PR, SC and RS.

In RS, rice is grown in approximately 130 municipalities (one million ha) located in the southern portion of the state, where census-based yield for 2014 was estimated as about 8 metric tons ha^{-1} (Figure 2a). In SC, rice is cultivated in about 85 municipalities (covering 150,000 ha), concentrated in the east portion, particularly the coastal region where yields are also high (6-8 metric tons ha^{-1}). Rice is broadly cultivated in PR but more intensely in small farms in the northwest region (in a total of 26,000 ha), where the production is targeted mainly for self-consumption.

Yields surveyed in Figure 2a are reported at the municipality level, but in most cases this might not be an accurate spatial representation because even if one single farm grows rice at a certain location, yield is reported for the entire municipality area. Therefore, a more detailed spatial distribution of harvested area of rice in southern Brazil is shown in Figure 2b, expressed as proportion of crop area in each grid cell (with a resolution of approximately 4 km x 4 km). The greatest proportion of rice occurs in two main regions: the coastal portions of RS and SC. Intense rice plantations are also observed in southeastern SC and through central and southern RS. In PR, areas with

relatively high proportion of grid cell occupied by rice are observed in the northwest and

south portions of the state.
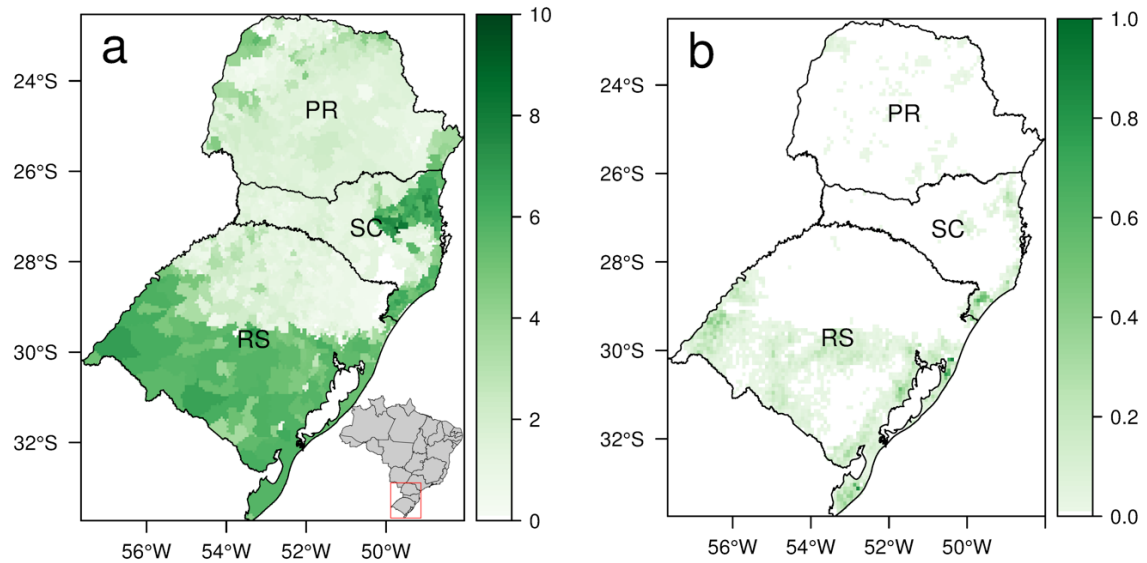
Figure 2. Geographical distribution in southern Brazil of (a) rice yield (in metric tons ha^{-1}), surveyed for year 2014 and (b) harvested area of rice, expressed as proportion of grid cell. Data from the Brazilian Institute for Geography and Statistics (2015) and Monfreda et al. (2008), respectively.

The most common soils where rice is grown are Planosols, characterized by a

slowly permeable horizon extending to the depth of 120 cm, and Gleysols with

hydromorphic properties in the first 50 cm of the surface (South-Brazilian Society for

Irrigated Rice, 2014). Climate suitability allows a wide range of sowing periods, but rice

is typically sown from early September to mid-December, depending on the cultivar.

Harvest usually takes place from February to April.

3.2   The Agro-IBIS model

Agro-IBIS is a crop model developed within the framework of the Integrated

BIosphere Simulator model – IBIS (Foley et al. 1996; Kucharik et al. 2000). IBIS is a

global dynamic vegetation model that represents a comprehensive range of terrestrial

biospheric processes, which are based on the land surface transfer (LSX) model (Pollard

& Thompson, 1995). IBIS simulates exchanges of energy, water, and carbon between the

land surface and the lower atmosphere, as well as vegetation dynamics and phenology,

and canopy physiology. Given the prescribed atmospheric forcing and soil properties, the

model predicts vegetation temperature, canopy air temperature and specific humidity.

Changes in soil temperature and moisture within the vertical soil column are

simulated using Fick and Darcy laws, respectively. Water reaching the soil is partitioned

into surface runoff and drainage, depending on soil physical properties such as porosity

and hydraulic conductivity. The surface flux of moisture depends on the atmospheric

boundary conditions and the characteristics of the land surface. Moisture exchange

between canopy and adjacent air is calculated using a resistance analog where the

potential is represented by the gradient between saturation vapor pressure of the canopy

and vapor pressure of the canopy air space. Similarly, water is withdrawn from the upper

soil layer into the air by direct evaporation when the pores of the soil are at or near

saturation.

Agro-IBIS shares the same physics as IBIS but additionally simulates crop

phenology, the effects of land use and agricultural management practices on crop yields

(irrigation, crop fertilization, crop rotation), and on the transport of chemical elements

such as inorganic nitrogen (N) through leaching (Kucharik, 2003; Kucharik & Brye,

2003). While the original version of Agro-IBIS simulated crop management for maize,

soybean and wheat, bioenergy crops have been recently included in the model

(Vanloocke et al. 2010, Cuadra et al. 2012). Agro-IBIS has been validated at the field and

regional scales for soil temperature (Kucharik & Twine, 2007; Kucharik, VanLoocke, Lenters, & Motew, 2013) and moisture in the United States (Soylu, Istanbulluoglu, Lenters, & Wang, 2011) and other sites around the world (Delire & Foley, 1999).

3.3   Description of the rice growth model

The rice growth model in Agro-IBIS was developed by analyzing and integrating the relationships between rice growth and environment through the use of published studies and field data. The model simulates rice phenology, photosynthesis, biomass accumulation and partitioning and yield in response to environmental factors and management practices. The rice growth model is based on the MACROS (Penning de Vries, Jansen, ten Berge, & Bakema, 1989) and ORYZA2000 (Bouman & Van Laar, 2006) models. In the next section I provide details on the parameterization of the rice growth model within the Agro-IBIS framework.

3.3.1   Calibration data

Agro-IBIS's rice phenology and biomass allocation algorithm were calibrated with a dataset collected from field experiments carried out at the experimental station of the Center for Temperate Climate unit of the Brazilian Agricultural Research Corporation (Embrapa) located in Capão do Leão, Rio Grande do Sul state (31°48'S, 52°24'W). For the phenology calibration, I used data which were previously collected by Embrapa technicians during the 2006/07 and 2007/08 growing seasons for the Taim and Querencia cultivars. In each season rice plants were sown in six different dates, covering all the typical sowing windows of the region. Over the course of each growing season,

development rates were calculated using the mean observed dates of emergence, panicle initiation, flowering and physiological maturity of ten randomly sampled plants of each variety.

In this field experiment, the total fresh weight of shoot, green leaves, dead leaves, stems and panicles was measured every 15 days. Samples were afterwards taken to greenhouse and maintained at a mean temperature of 50ºC for about 5 days to obtain the dry weight of the biomass samples. Allocation coefficients were estimated based on the proportion of the weight of each organ to the total plant weight over the growing season. Leaf Area Index (LAI) was measured with a LAI-2000 plant canopy analyzer (Li-Cor, lnc., Lincoln, NE). I also assess model performance at the International Rice Research Institute (IRRI) in the Philippines (14°11'N, 121°9'E), using growth rates and LAI and biomass measurements from the cultivar IR72 in the wet season of 1991 (Castañeda, Bouman, Peng, & Visperas, 2002) that are available at the Oryza2000 website[1]. A summary of the experiments, the variables reported, and their use within this study is presented in Table 2.

Table 2. Experimental data for used in this study for model calibration and evaluation

Location	Description	Measured variables	Used for
The Embrapa Temperate Climate experimental station, Rio Grande do Sul, Brazil	Growing seasons of 2006/07 and 2007/08, multiple planting dates	Duration of growth stages, bi-weekly relative weights of stem, leaf and panicle	Calibration of development rates and carbon allocation fractions
	Growing season of 2014/15, multiple planting dates	Stem, leaf and panicle biomass; leaf area index	Model evaluation
The IRRI farm, Los Baños, Philippines	Wet season of 1992. Planting on 1 Jul 1992, maturity on 14 Oct 1992	Stem, leaf and panicle biomass; leaf area index	Model evaluation

3.3.2 *Thermal accumulation and growth phases*

In the new Agro-IBIS rice formulation, as in most crop models, the main environmental force driving phenological development of rice is temperature. The temperature-based growth function for rice assumes that the rate of progression through each phase is related to daily mean temperature above a base temperature up to an optimum temperature, beyond which the rate decreases, until a maximum temperature is reached (Kiniry, Rosenthal, Jackson, & Hoogenboom, 1991). Development rate is zero for temperatures below the base temperature or above the maximum temperature. Following Bouman et al. (2001), hourly heat units for plant development (HHU, in °Cd h^{-1}) are calculated as:

$$HHU = \begin{cases} 0 & \text{for } T_{air} \leq T_{base} \text{ or } T_{air} \geq T_{high} \\ (T_{air} - T_{base})/24 & \text{for } T_{base} < T_{air} \leq T_{opt} \\ \dfrac{T_{opt} - (T_{air} - T_{opt}) \times \dfrac{(T_{opt} - T_{base})}{(T_{high} - T_{opt})}}{24} & \text{for } T_{opt} < T_{air} < T_{high} \end{cases} \tag{1}$$

where T_{air} is the hourly mean air temperature, T_{base}, T_{high} and T_{opt} are, respectively, the base temperature, the maximum temperature and the optimum temperature for phenological development, all in degrees Celsius. The daily increment in heat units (DHU, in °Cd d^{-1}), which is effectively used for growth calculations, integrates HHU over the course of every simulation day in the growing season, as indicated below:

$$DHU = \sum_{h=1}^{24} (HHU) \tag{2}$$

The crop development rate (DVR_C, in $°Cd^{-1}$) of rice is calculated based on a simple product of the daily heat units by a development rate constant (DVR_{phase}) of each growing phase:

$$DVR_c = DHU \times DVR_{phase} \qquad (3)$$

where the development rate constant DVR_{phase} is the inverse of the temperature sum required to complete a specific phase. For example, the DVS range for the basic vegetative phase (i.e. 0.3) divided by the total daily heat accumulation during that growing phase yields the development rate constant for that phase.

Rice growth is affected by day length (which is a function of latitude and time of the year) during the photo-period sensitive phase (Vergara & Chang, 1985), whose effect is translated into crop growth as a multiplication factor to the development rate DVR_c of that phase. Therefore, sub-optimal photoperiod (or day length) will result in a longer photoperiod-sensitive phase.

The development stage (DVS) of rice, which defines the crop's physiological age, is the integration of DVR_c over the growing season:

$$DVS = \sum_{phase=1}^{4} DVR_c \qquad (4)$$

Our model assumes four phenological phases for rice, viz: i) basic vegetative phase (BVP), from emergence (DVS=0) to the start of the photoperiod-phase (DVS=0.3), ii) photoperiod-sensitive phase (PSP), from DVS=0.3 until panicle initiation (DVS=0.5), iii) panicle formation phase (PFP), from DVS=0.5 until 50% flowering (DVS=0.75) and iv) grain-filling phase (GFP), from DVS=0.75 until physiological maturity (DVS=1). These DVS thresholds are based on those defined by Bouman et al. (2001) but rescaled to

fit the Agro-IBIS framework. The development rate coefficients used in the simulations

are shown in Table 3.

Table 3. Description of the rice growth stages and development rate coefficients used in this study. Values adjusted based on data from the field experiments described in section 3.3.1.

Growth phase (and its equivalence to the growth stages proposed by Counce *et al.*, 2000)	Description	Development stage (DVS) range	Crop development rate constant – DVR_C ($°C$ day^{-1})	
			Brazil	Philippines
Basic vegetative (EM - V6)	Emergence to start of photoperiod-sensitive phase	0 – 0.3	0.000920	0.0008860
Photo-period sensitive (V6 – R0)	End of basic vegetative stage to panicle initiation	0.3 – 0.5	0.000628	0.0006876
Panicle formation (R0 – R4)	Panicle initiation to 50% flowering	0.5 – 0.75	0.000567	0.0005210
Grain filling (R4 – R9)	50% flowering to physiological maturity	0.75 – 1.0	0.000684	0.0089910

As mentioned before, development rate coefficients were derived based on the

thermal accumulation during each growth phase. Let's consider for example the basic

vegetative phase (BVP) at the Brazilian site. The observed BVP duration was 31 days,

and the heat accumulation during that period of time was 326.83 $°Cd^{-1}$. The quotient

between the DVS range for that growth phase (i.e. 0.3) and the total heat accumulation

yield (326.08 $°Cd^{-1}$) yields a development rate of 0.000920 $°C$ day^{-1} for that growth stage

(Table 3).

Additionally, new model variables are introduced to represent the length of each phenological phase in order to allow an accurate comparison with field observations. Figure 3 shows an example of the temporal evolution of DVS in southern Brazil over the 2006/07 growing season and the approximate duration of the vegetative (31 days), photo-period (31 days), panicle formation (34 days) and grain filling (36 days) phenological phases. Maturation is reached 132 days after emergence day (November 10, 2006 for this simulation).
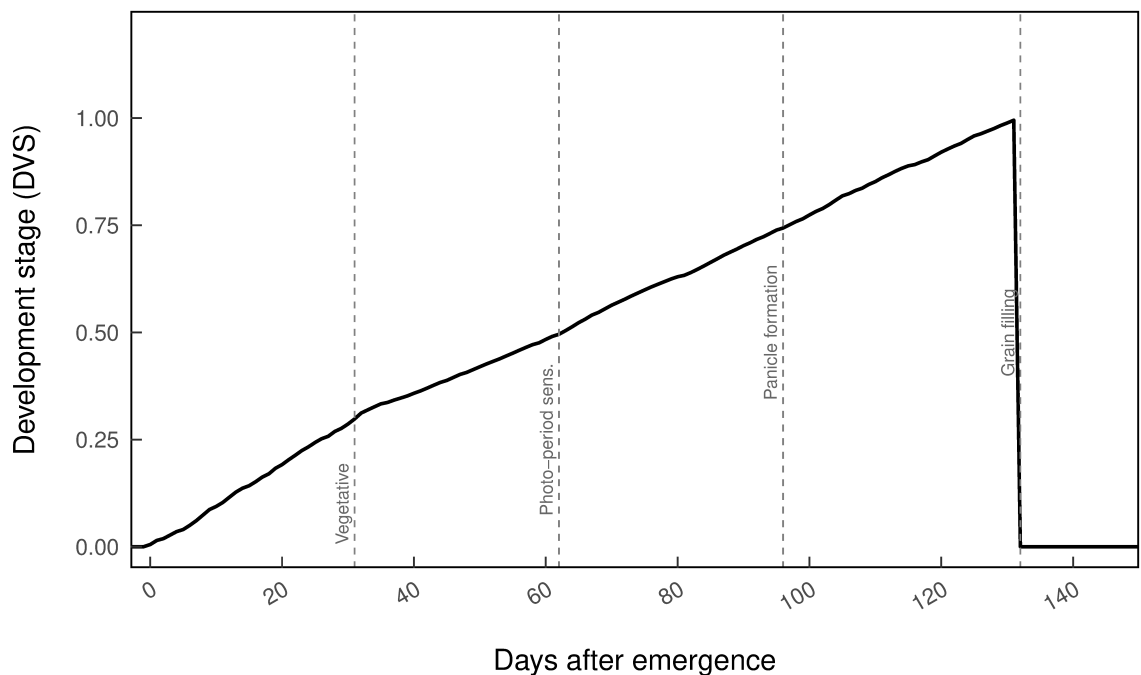
Figure 3. Time course (days after emergence, DAE) of the rice development stage (DVS, unitless) simulated by Agro-IBIS over the 2006/07 growing season. Vertical dashed lines represent the end of each phenological phase of rice growth. Maturity is reached when DVS is equal to 1.

3.3.3 CO$_2$ assimilation by the canopy

In Agro-IBIS, the daily canopy assimilation rate is calculated by integrating the instantaneous leaf photosynthesis rates over the height of the canopy and over the day.

24

The Agro-IBIS photosynthesis module is based on the formulations by Farquhar et al. (1980). For C_3 crops, the gross photosynthesis rate per unit leaf area, A_g (in mol CO_2 m^{-2} s^{-1}) is determined by three limiting factors, Rubisco, light, and sucrose synthesis, as follows:

$$A_g = min(J_c, J_e, J_s) \tag{5}$$

where J_c represents the Rubisco-limited rate of photosynthesis, J_e is light-limited rate of photosynthesis, and J_s is the photosynthesis limited by the inadequate rate of utilization of triose phosphate. The variables J_c, J_e and J_s are given by:

$$J_c = \frac{V_m(C_i - \Gamma_*)}{C_i + K_c\left(1 + \frac{[O_2]}{K_o}\right)} \tag{6}$$

$$J_e = \alpha_3 Q_p \left(\frac{C_i - \Gamma_*}{C_i + 2\Gamma_*}\right) \tag{7}$$

$$J_s = V_m/2.2 \tag{8}$$

where V_m is the carboxylase capacity of Rubisco (mol CO_2 m^{-2} s^{-1}), C_i is the concentration of CO_2 in the intercellular air spaces of the leaf (mol mol^{-1}), Γ_* is the compensation point for gross photosynthesis (mol mol^{-1}), K_c and K_o are the Michaelis-Menten coefficients (mol mol^{-1}) for CO_2 and O_2, respectively, $[O_2]$ is the concentration of O_2 in the intercellular air spaces of the leaf (mol mol-1), α_3 is the intrinsic quantum efficiency for CO_2 uptake in C_3 plants (mol CO_2 mol^{-1} quanta) and Q_p is the flux density of photosynthetically active radiation absorbed by the leaf (mol quanta m^{-2} s^{-1}).

The net daily dry matter accumulation is obtained by subtracting the maintenance respiration requirements from A_g. For crops, the daily net dry matter produced is partitioned among the various plant organs (roots, leaves, stem and reproductive organs,

25

which in rice are panicles). Specifically for rice, the allocation coefficients are dynamically determined as a function of the crop's physiological age (DVS) using a base temperature of 11°C (Streck et al., 2007), as described in the next section.

3.3.4   *Carbon allocation*

Several modifications were made to the dynamic crop module to better fit it into the coupled regional model framework. The Agro-IBIS allocation coefficients for rice were derived from experimental growth data and depend on the phenological development stage of the plant (DVS – see section 3.3.2). Figure 4 shows the simulated and observed fractions of carbon partitioned to each organ (see section 3.3.1 for details on the field study that originated the observed allocation patterns). Generally, the largest share of biomass is initially attributed to roots and leaves, then to stems as the plant ages, and ultimately to the reproductive organs when grain fill begins.
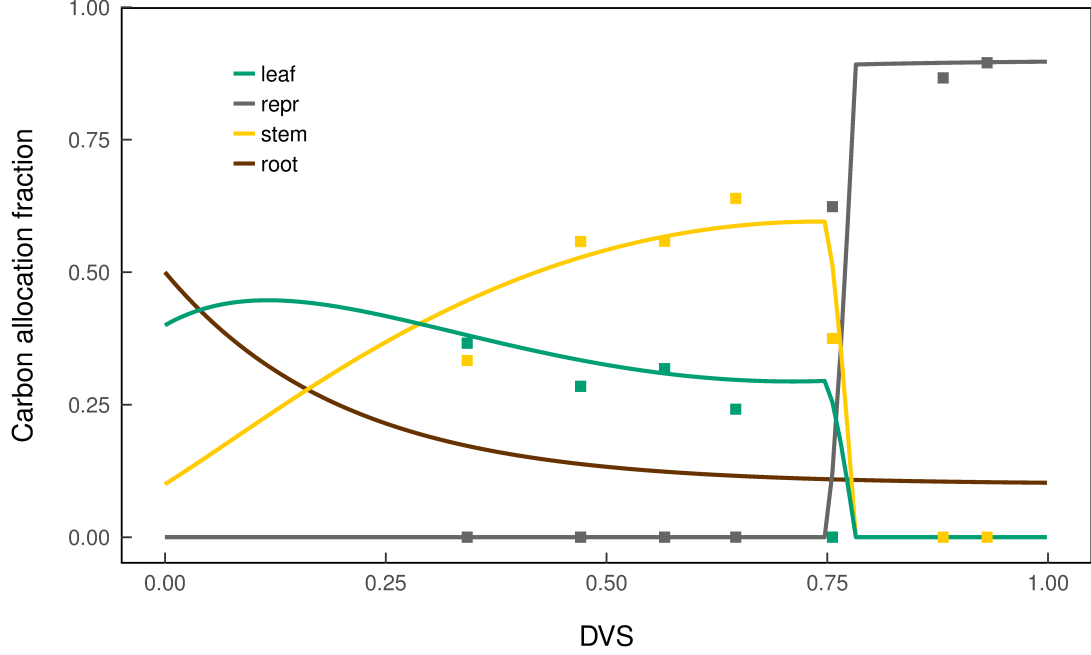
Figure 4. Simulated (lines) and observed (squares) patterns of carbon partitioning to the different organs in rice as a function of development stage. Colors represent allocation fractions to roots (brown line), leaves (green line), stems (yellow line) and grains (gray line).

The partitioning function for the carbon allocated to the roots is expressed as:

$$f_{root} = (root_i - root_f)e^{-a \times DVS} + root_f \qquad (9)$$

where $root_i$ and $root_f$ are parameters that define the initial and final allocation fractions reserved to the roots, respectively, and a is a parameter that controls the rate of decline between $root_i$ and $root_f$. The fraction allocated to the reproductive organs is defined as:

$$f_{repr} = (1 - f_{root})\left(\frac{e^{DVS \times b}}{e^{DVS_{repr} \times b}} - 1\right) \qquad (10)$$

where DVS_{repr} is the DVS value where biomass starts to be allocated to reproductive organs (assumed here as 0.75) and b is a parameter that controls the slope of the allocation line to the reproductive organs.

The fraction allocated to the stems is calculated as:

27

$$f_{stem} = (1 - f_{repr} - f_{root}) [(Q \times DVS^2) + (L \times DVS + I)] \qquad (11)$$

where Q, L and I are parameters that define the shape of the allocation curve to stems. The values of the parameters a, b, Q, L and I used in this study to produce the allocation curves shown in Figure 4 are summarized in Table 4.

Table 4. Parameter values used to create the allocation curves.

Parameter	Value
a	5
b	22
Q	-0.9
L	1.3
I	0.2

Last, the fraction allocated to the leaves is defined as the remainder of the other allocation fractions:

$$f_{leaf} = 1 - f_{stem} - f_{repr} - f_{root} \qquad (12)$$

Leaf area index increment is then calculated daily as the product of the dry matter allocated to leaves and specific leaf area. Crop yield is calculated from the quotient of total dry weight of the reproductive organs at maturity and the fraction of grain dry matter that is carbon (usually assumed as 45%).

3.3.5 *Growth inhibitors*

In Agro-IBIS, V_{max} is a parameter that indicates the maximum carboxylase capacity of Rubisco at 15°C and without water or heat stress. During periods of low precipitation, however, soil moisture may become too low to meet the evaporative demand imposed by the atmosphere. Plant leaves then lose turgor and stomata close to prevent further moisture losses to the environment. As a result, the entry of CO_2 into the

leaf is constrained and photosynthesis, crop growth (i.e. leaf development) and yield are reduced. Similarly, temperature is also a factor known to negatively affect rice growth. Temperature influences rates of physiological processes that govern plant growth (Hatfield & Prueger, 2015; Prasad et al., 2006).

Typically, photosynthesis increases with increasing temperature until a crop specific optimum temperature is reached, and increases in temperature beyond this optimum threshold decrease photosynthesis rate (Jagadish et al., 2007). Thus, the following equation is used in Agro-IBIS to simulate the actual carboxylation rate (V_m) by considering the reduction of the maximum carboxylase capacity due to temperature dependency and under limiting water supply:

$$V_m = V_{max} D_s T_{vm} \qquad (13)$$

where D_s and T_{vm} are, respectively, the drought and temperature stress coefficients that constrain the carboxylase capacity of Rubisco. The drought stress factor (D_s), which limits the photosynthesis rate by simulating stomatal closure, is calculated by accounting for water availability in the soil:

$$D_s = 1 - \left[\frac{\log\left(1 + (799\,e^{-12\,awc})\right)}{\log 800} \right] \qquad (14)$$

where *awc* is the available water fraction in the soil column following Campbell & Norman, 1998, weighted by the root distribution fraction (froot):

$$awc = \sum_{i=1}^{n} \frac{\theta_i - \theta_{wilt_i}}{\theta_{field_i} - \theta_{wilt_i}} \times froot_i \qquad (15)$$

where θ is the soil moisture content (fraction of pore space) and θ_{field} and θ_{wilt} indicate the moisture contents at field capacity and wilting point, respectively. For a silty clay loam soil (Figure 5), the Agro-IBIS drought stress factor starts limiting photosynthesis

when soil moisture content reaches ~70%. At 50% soil moisture content, photosynthesis happens at only 25% of its potential rate.
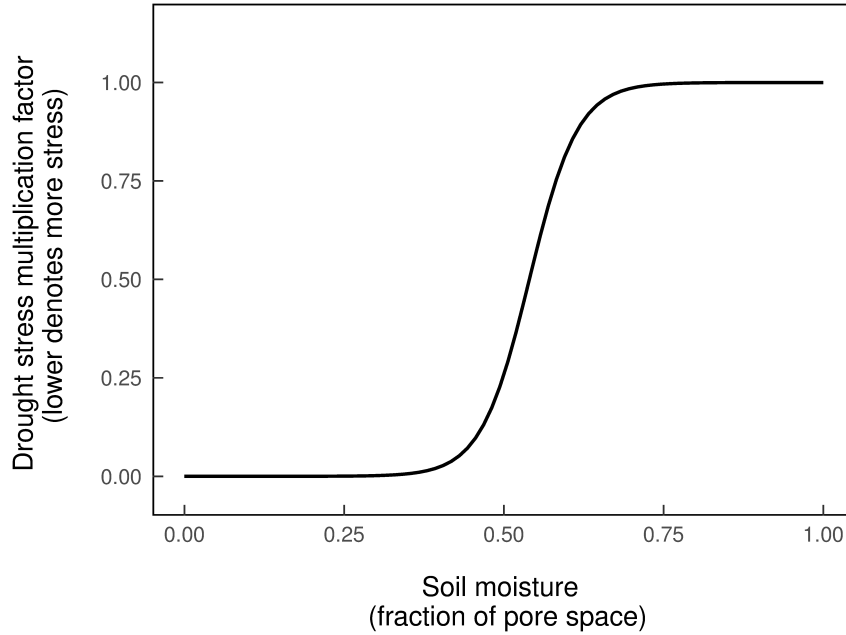
Figure 5. The relation between the soil water content and the drought stress multiplication factor on the carboxylation rate of rice.

The temperature stress factor (T_{vm}) is defined as a modified version of the Collatz conductance model (Collatz, Ribas-Carbo, & Berry, 1992):

$$T_{vm} = \frac{Q_{10}^{\frac{T_l - 15}{10}}}{(1 + e^{f_1(T_{low} - T_l)})(1 + e^{f_2(T_l - T_{high})})} \qquad (16)$$

where Q_{10} is the proportional increase in a parameter value for a 10°C increase in the temperature, T_l is leaf surface temperature (°C), and f_1, f_2, T_{low} and T_{high} are parameters that adjust the curve shape of the function. A curve showing how Agro-IBIS's V_m responds to temperature, considering parameters T_{low} and T_{high} adjusted for rice based on recent literature reports (Hatfield & Prueger, 2015; Sánchez, Rasmussen, & Porter, 2014), is provided in Figure 6. The maximum V_m is found to be at 31-33°C, which is consistent with the responses reported by Makino et al. (1994) and Nagai and Makino (2009).
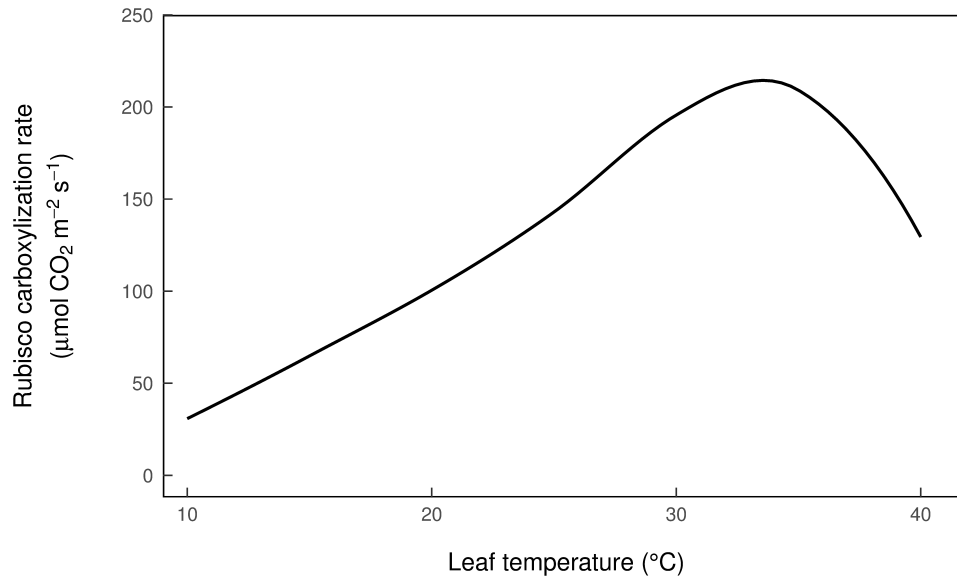
Figure 6. Modeled carboxylation rate plotted as a function of leaf temperature using Agro-IBIS' V_m equation parameterized to the rice plant function type within the model.

3.4   Description of the rice irrigation model

Although the original Agro-IBIS formulation had a general scheme to determine irrigation needs for maize, soybean and wheat based on soil moisture (Kucharik, 2003; Kucharik et al., 2000; Kucharik & Brye, 2003), the irrigation algorithm for rice presented here is a complete new model, specifically designed for a paddy environment. The new Agro-IBIS water balance of a puddled rice field is based on FAO's irrigation recommendations for rice (Brouwer et al., 1989), which were also implemented in the Oryza2000 model (Bouman et al., 2001; Bouman & Van Laar, 2006).

The volume of water required by rice irrigation is defined as the sum of the water required to flood the soil and produce a water layer at the beginning of the growing season plus the water amount required to maintain a minimum water layer (i.e. compensate losses by evapotranspiration, percolation and runoff). The irrigation

31

approach incorporated into the Agro-IBIS rice model is conceptually illustrated in Figure 7.
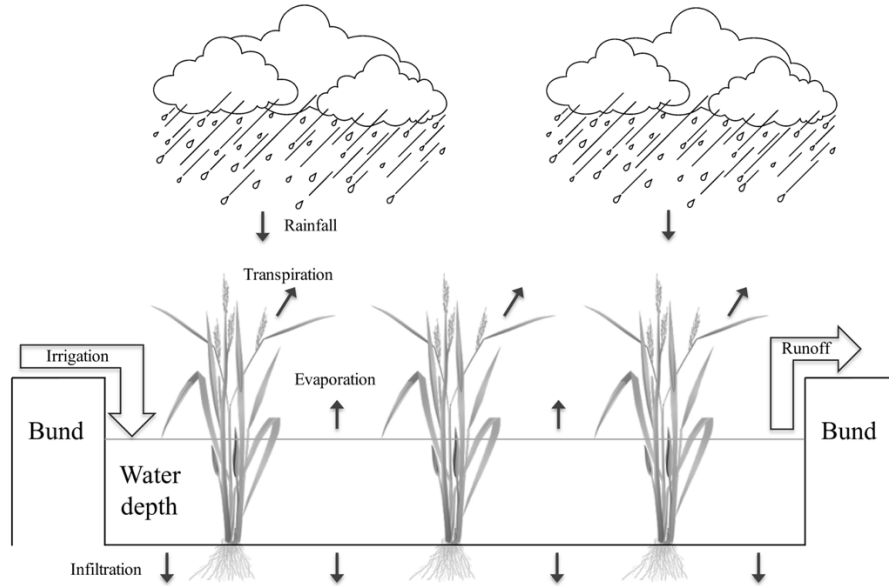
Figure 7. Water balance of a lowland rice field as implemented in Agro-IBIS. In this scheme, demand for irrigation begins when the ponded water depth drops below a specified minimum level, which is prescribed to the model based on the local management practices of the study region.

In the first day of the growing season (i.e. the same day when rice is planted), an initial amount of irrigation is provided to make up the initial ponded water level. Then, on an hourly basis and over the growing season, the new Agro-IBIS paddy formulation keeps track of gain (precipitation) and losses (evaporation, transpiration and infiltration) of water in the system to determine changes in the depth of the water layer. Therefore, the depth variation of the initial water layer is controlled according to the expression:

$$\Delta WD = P - E - T - I \tag{17}$$

where ΔWD represents change in the ponded water depth (kg m^{-2} h^{-1}), P is the precipitation rate at the ground (kg m^{-2} h^{-1}), E is evaporation (kg m^{-2} h^{-1}), T is

transpiration (kg m^{-2} h^{-1}) and I is infiltration (kg m^{-2} h^{-1}). Here, the infiltration term is defined as the amount of water in the first (i.e. the most superficial) layer of the soil that is flowing down through the soil column. No horizontal flows (i.e. seepage towards the paddy bund) are considered by the irrigation model.

Once the water balance at the surface has been solved, if water losses surpasses rainfall input so that the depth of the ponded water drops below to a minimum specified level, irrigation is applied by the model to ensure the maintenance of the minimum water depth in the field, therefore preventing yield losses caused by absence of sufficient water for growth (Anbumozhi, Yamaji, & Tabuchi, 1998). On the other hand, any water in excess of bund height is assumed to leave the paddy as surface runoff. Initial, minimum and maximum water levels are specified to the model as parameters. Hourly demand for irrigation is integrated on a daily basis under the assumption that water supply takes place only between 6am and 6pm and throughout the growing season.

The demand for irrigation (D_{irrig}, in mm h^{-1}) is equal to the difference between the timestep water level and the specified minimum threshold, according to the expression:

$$D_{irrig} = \begin{cases} WH_{min} - WH_{cur}, & \text{if } WH_{cur} < WH_{min} \\ 0, & otherwise \end{cases} \qquad (18)$$

where WH_{min} is the minimum water layer height (mm) and WH_{cur} is the current timestep water layer height (mm).

Total daily irrigation (mm d^{-1}) is then the cumulated demand for irrigation within a 12-hour period, assuming irrigation takes place only between 6 a.m. and 6 p.m.:

$$IRRIG_{day} = \sum_{i=6a.m.}^{6\ p.m.} D_{irrig\ i} \qquad (19)$$

The seasonal irrigation demand (SID) index is defined as the daily irrigation integrated over the entire growing season (i.e. from planting to harvest):

$$SID = \sum_{i=planting\ day}^{harvest\ day} IRRIG_{day} \qquad (20)$$

The volumetric water demand (VWD, in m^3) is determined by multiplying SID in each grid cell by the area of the grid (weighted by the fraction of grid cell covered with rice) and integrating it over a region:

$$VWD = \sum_{study\ region} (SID \times area_{grid} \times fraction_{rice}) \qquad (21)$$

where SID is expressed in mm (or l m^{-2}), the area of the grid is expressed in km^2 and fraction of rice was derived from a global dataset that compiles harvested area of 175 crops around the world for the year 2000 (Monfreda et al., 2008). The changes in VWD under each climate scenario, in each state and for the whole region, were analyzed.

3.5   Model validation

In order to evaluate Agro-IBIS' ability to predict rice phenology, I conducted two types of assessment. The first assessment was conducted at the experimental site in southern Brazil described in Section 3.3.1. In this assessment, the predicted durations of the growth stages were compared to observations from the 2006/07 and 2007/08 growing seasons. The second assessment was conducted for both the Brazilian and Philippine validation sites. The simulated LAI and biomass of leaves, stems and panicles were compared against observations of the 2014/15 growing season for southern Brazil and the 1992 wet season for Philippines. In both assessments I performed regional Agro-IBIS simulations over southern Brazil and Philippines forced with the CRU TS v.4.0 monthly

34

climate dataset (Harris, Jones, Osborn, & Lister, 2014), and analyzed output data

extracted from the grid cell closest to the coordinates of each experimental site (31.63°S

and 52.43°W in southern Brazil and 14.22°N, 121.25°E in Philippines).

Due to lack of irrigation measurements at the field scale in the study region, I

evaluate the model by comparing the combined evaporation and transpiration

components of Agro-IBIS with evapotranspiration (ET) measurements by Timm et al.

(2014). Although previous studies have validated Agro-IBIS' representation of water

fluxes (El Maayar et al., 2001; El Maayar, Price, Black, Humphreys, & Jork, 2002), this

assessment was intended to check whether Agro-IBIS realistically simulates the water

flux in the study region. I also check the timing of irrigation application by plotting a

time series of precipitation, evapotranspiration and drainage, and irrigation.

3.6   Experimental design for the future runs

Possible changes in rice irrigation, phenology and yield are investigated with a

multi-model ensemble from the fifth phase of the Coupled Model Intercomparison

Project (CMIP5 - Taylor et al. 2012). Model simulations from CMIP5 provide the basis

for the Fifth Assessment Report (AR5) of the Intergovernmental Panel on Climate

Change. Both the "medium-emission" and "high-emission" Representative Concentration

Pathways (i.e. "RCP4.5" and "RCP8.5") are used. In these scenarios, radiative forcing

increases throughout the twenty-first century until reaching a level of 4.5 W m^{-2} and 8.5

W m^{-2}, respectively, at the end of the century (van Vuuren et al., 2011). Although other

scenarios are available in CMIP5, RCP4.5 and RCP8.5 are used here to examine

potentially impacts of "medium" and "extreme" climatic changes in rice production.

I analyzed the period encompassing January 1 2011 to December 31 2100, which was partitioned into 30-year mean sub-periods: near future, from 2011 to 2040, mid-century, from 2041 to 2070 and far future, from 2071 to 2100. Each 30-year mean period was compared to the current climate period 1981-2010. Monthly averages of the following surface variables were used as input for Agro-IBIS: precipitation, air temperature and relative humidity at 2 m height, surface winds at 10 m height and cloudiness. Monthly averages were downscaled to daily and hourly averages by the weather generator within Agro-IBIS, which is based on the WGEN model (Richardson & Wright, 1984). Based on data availability of required variables to drive Agro-IBIS, temporal resolution and availability at the time of data collection, five CMIP5 models were chosen for each emission scenario. Table 5 lists the detailed information of the models used in this study.

Table 5. List of CMIP5 global models used in this study

Model acronym	Modelling Centre (Country)	Atmospheric Component resolution (lat/lon, °)
CanESM2	Canadian Centre for Climate Modelling and Analysis (Canada)	2.8 x 2.8
GFDL-ESM2M	NOAA Geophysical Fluid Dynamics Laboratory (USA)	2.0 x 2.5
NorESM1-M	Norwegian Climate Centre (Norway)	1.9 x 2.5
INMCM4	Institute for Numerical Mathematics (Russia)	1.5 x 2.0
MRI-CGCM3	Meteorological Research Institute (Japan)	1.1 x 1.1

All CMIP5 model outputs were reprojected, regridded to a half degree cell (compatible with Agro-IBIS surface datasets) and bias corrected. Bias correction was performed with the quantile mapping technique (Gudmundsson, Bremnes, Haugen, & Engen Skaugen, 2012), using data from the Climate Research Unit (CRU TS v.4.0; Harris et al. 2014). I use CRU monthly observations of current climate (1981-2010) as the baseline period to correct the CMIP5 historical data, and these corrections are then applied to the future projections to provide bias-corrected future climate data. Agro-IBIS was then forced with bias-corrected CMIP5 data, in a total of ten simulations (five models per each emission scenario). The results presented here are based on the ensemble mean of the five models. The appendix chapter presents a brief examination of the bias correction outcome, as well as an assessment of the models' ability to correctly simulate spatial patterns of observed present-day climate data in southern Brazil.

Additional input data needed to drive Agro-IBIS consist of soil texture class at each model soil layer and atmospheric CO_2 concentration. In the irrigation runs, I assume a crop management practice where the soil is flooded from planting to harvesting. Since rice typically grows in soils with good water holding capacity (South-Brazilian Society for Irrigated Rice, 2014), the soil texture was set aiming to prevent high water losses through drainage. Thus, soil texture class is set as silty clay loam for the top five layers and clay for the remaining six layers across the study domain in order to limit drainage to about 2 mm d^{-1} (Bouman et al., 2007). The profile, textural, and water-holding properties of the soil column in the simulations are summarized in Table 6.

Table 6. Soil parameters used for the Agro-IBIS simulations. Data from Rawls et al. (1992).

Soil depth (cm)	Soil texture	Sand/silt/clay (fraction)	Porosity (volume fraction)	Saturated hydraulic conductivity (cm h^{-1})
0-100	Silty clay loam	0.09/0.58/0.33	0.471	0.15
100-250	Clay	0.20/0.20/0.60	0.475	0.06

Based on typical management practices in southern Brazil (South-Brazilian Society for Irrigated Rice, 2014), it was assumed in all simulations that a water layer of 70 mm is established at the day of emergence . It was also assumed that the minimum water layer (i.e., the threshold for irrigation) is 30 mm. Emergence dates for rice were set to November 10th (Julian day 314) in all simulations, and harvest day was determined automatically by the model once grain maturity was achieved.

Rice irrigation was also performed in the phenology runs, in order to prevent yield losses due to drought stress and to isolate the effects of temperature and CO_2 only. For future scenario simulations Agro-IBIS was forced with the bias-corrected output from the five CMIP5 models described in section 3.6. Two sets of simulations were performed:

1. STA-CO_2 – with CO_2 fixed at 380 ppm in order to exclude any effects from CO_2 fertilization in the future. This procedure allows us to estimate the effect of climate change alone on yield.

2. DYN-CO_2 – includes both dynamic CO_2 and a changing climate, in order to represent their combined effects on crop yield.

In the DYN-CO_2 simulations, the CO_2 concentrations used to simulate the CO_2 fertilization effect were taken from the CMIP5 dataset (http://tntcat.iiasa.ac.at/RcpDb/dsd?Action=htmlpage&page=download). The historical

part of the CMIP5 concentrations dataset (1860–2005) is derived from a combination of

observed sources (ice core and marine and atmospheric observation sites). From 2005 on,

CO_2 concentrations recommended for CMIP5 were calculated for the 21st century based

on harmonized CO_2 emissions of the integrated models that underlie the RCPs. Figure 8

shows the evolution of CO_2 concentrations as observed in the 20th century and projected

in the 21st century simulations in the two RCP scenarios considered in this study. Both

scenarios assume continued growth in atmospheric levels of greenhouse gases for the

next few decades. Carbon dioxide emissions in RCP4.5 peaks at about 540 ppm CO_2 in

year 2100, while RCP8.5 assumes higher emissions, peaking at 940 ppm CO_2 in year

2100.
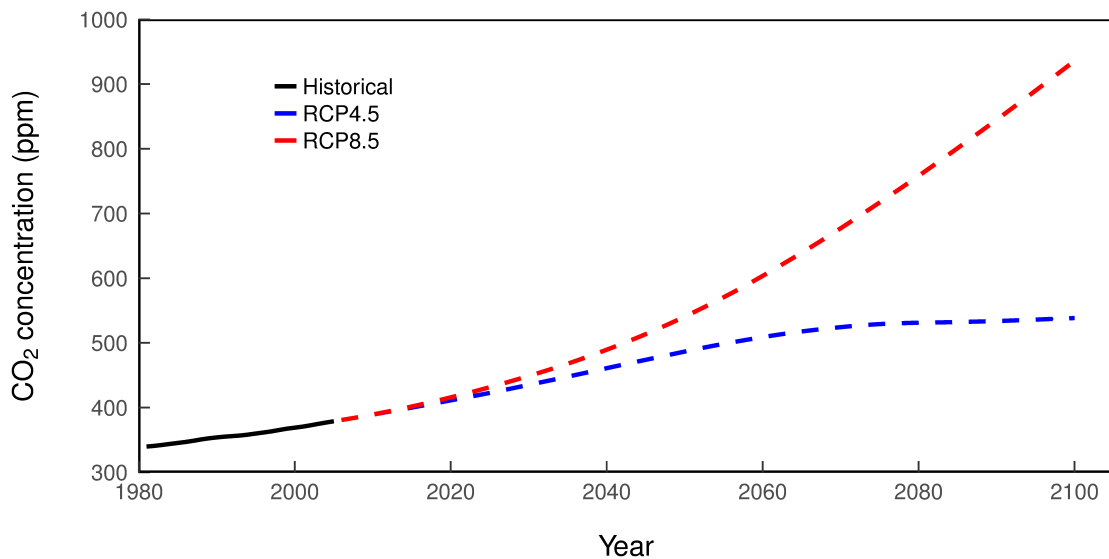
Figure 8. The time evolution of the CO_2 concentrations used to drive Agro-IBIS in the
future climate experiments.

Chapter 4. Results and discussion

In this chapter I first present the main findings of the rice growth (section 4.1) and irrigation models (section 4.2) assessment in current climate, and then discuss how climate change potentially translates into impacts on rice phenology and yield (section 4.3) and irrigation requirements (section 4.4).

4.1 Rice growth evaluation

4.1.1 Rice phenology in current climate

Because many physiological and morphological processes change according to the phenological stage of the plant, an accurate description of phenological development of a crop plant is essential. A comparison of the observed and simulated durations of the rice growth stages for the 2006/07 and 2007/08 growing seasons in southern Brazil are shown in Figure 9. Agro-IBIS predicted the duration of each stage based on the development rates calculated using the observed crop phenology data from the field experiment, i.e. emergence dates, panicle initiation, flowering, and physiological maturity (see Table 3).
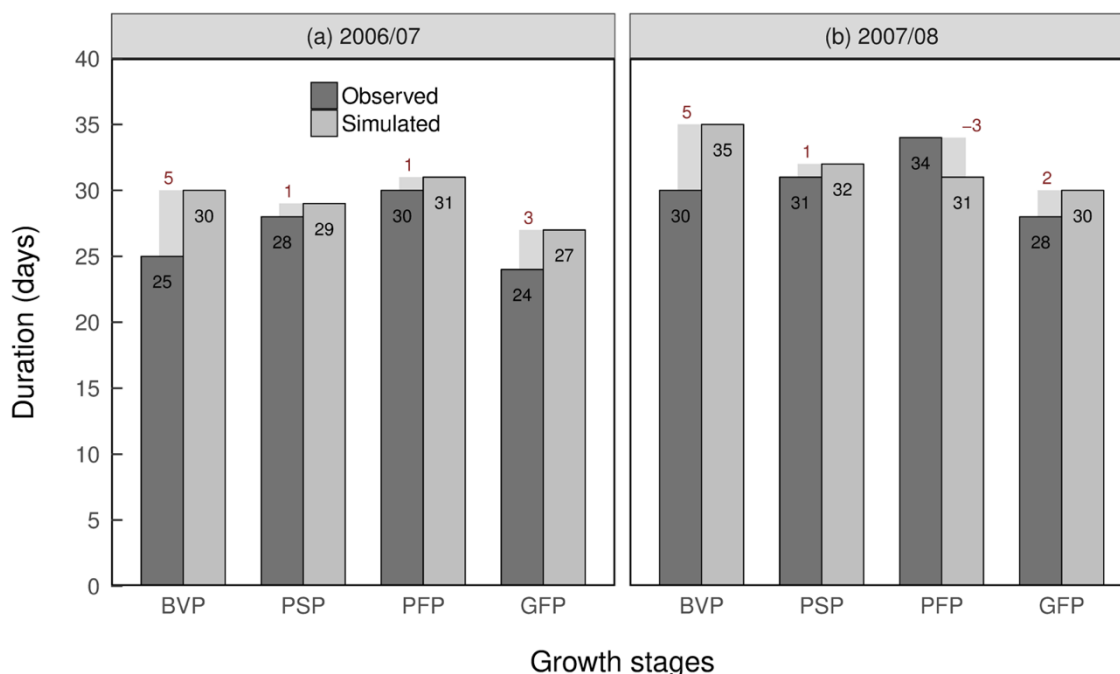
Figure 9. Comparison of observed and simulated duration of the growth phases of rice for the growing seasons of (a) 2006/07 and (b) 2007/08 in southern Brazil. Red denotes the difference (simulated minus observed) in days. The acronyms on the x-axis are defined as follows: Basic Vegetative Phase (BVP), Photoperiod-Sensitive Phase (PSP), Panicle Formation Phase (PFP) and Grain Filling Phase (GFP).

The simulations showed that Agro-IBIS tends to overestimate the duration of every growth stage, except for the panicle-filling phase of the 2007/08 growing season where the model underestimated the observed duration by three days. Lowest and largest differences were observed in the photo-sensitive (PSP) and basic vegetative (BVP) phases, respectively. Observed and simulated growing season length were 107 and 117 and 123 and 128 days for the growing seasons of 2006/07 and 2007/08, respectively. The growing cycle of 2006/07 was shorter than that of 2007/08 because of higher temperatures observed in that season (Figure 10).
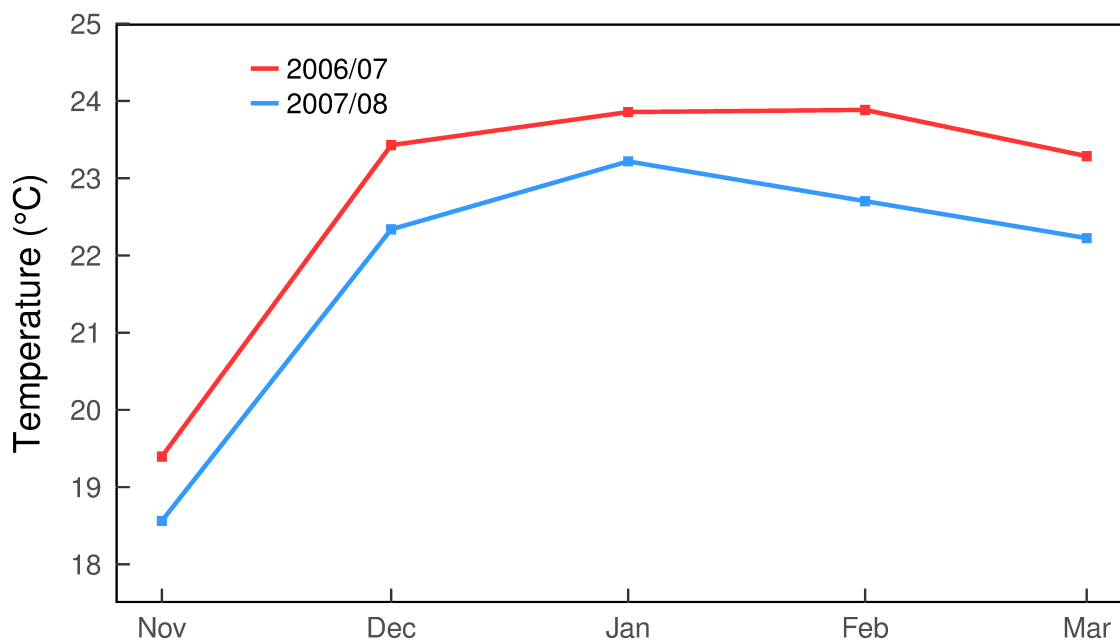
Figure 10. Agro-IBIS simulated mean monthly temperature for the rice growing seasons of 2006/07 and 2007/08 at the experimental site in southern Brazil.

4.1.2 Leaf area index and biomass

In this section, Agro-IBIS' ability to simulate net carbon uptake by rice during growing periods was tested by comparing the temporal changes in leaf area index (LAI) and biomass between simulations and observations. A comparison between simulated and measured crop growth variables for the experiments in Brazil and Philippines is show in Figure 11. In both locations, the dynamics of leaf area index (LAI) and biomass of leaves, stems, and grains was realistically simulated. Agro-IBIS accurately captured the increase in rice LAI in both sites, and simulated a peak LAI of 8.1 in southern Brazil (Figure 11a) and 4.8 in Philippines (Figure 11c). However, the model showed a tendency to reach maximum LAI values too early in the season (three days in Brazil and five days in Philippines), which is thought to be caused by a premature end of carbon allocation to

leaves. Upon maturity, Agro-IBIS simulates leaf senescence through a simple function that linearly decreases LAI until harvest.
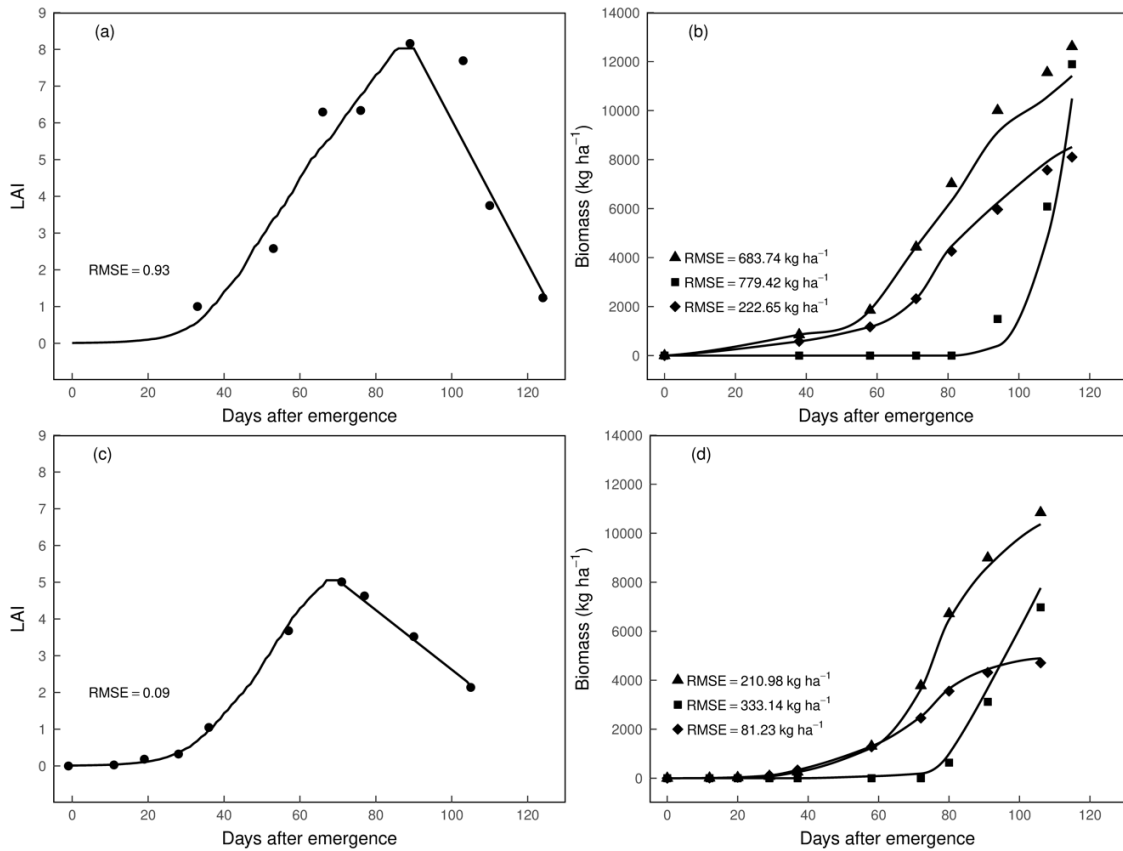
Figure 11. Simulated (lines) and measured LAI (●), total dry matter of leaves (♦), stems (▲) and grains (■) for (a and b) the 2014/15 growing season in Rio Grande do Sul, Brazil; and (c and d) the wet season of 1992 in Philippines.

In both southern Brazil and Philippines, the dynamics in biomass of leaves, stems, and grains was captured quite well by Agro-IBIS. At the Brazilian site, the model appears to have a bias towards underestimating the biomass of stems and grains, particularly at the end of the season (Figure 11b). Biomass of leaves, on the other hand, tended to be overestimated by the model but with a lower bias. At the Philippine site, Agro-IBIS also underestimated the biomass of stems and overestimated the biomass of leaves (Figure 11d). The errors for end-of-season biomass at the Brazilian site were 5.1%, -9.5% and -

43

11.8% for leaves, stems and grains respectively, and 3.9%, -4.4% and 11.3% for the Philippine site.

4.2 Irrigation assessment

A comparison between observed and modeled ET at a paddy field in southern Brazil is shown in Figure 12. Agro-IBIS overestimates ET in the vegetative (early six weeks) and ripening (last four weeks) stages. During the reproductive stage, the model reproduces ET reasonably well. Over the growing season (DOY 316 to 73), RMSE was 1.04 mm day^{-1}, total observed ET was 584 mm and total modeled ET was 645 mm. Overall, Agro-IBIS realistically reproduces the seasonal ET pattern captured in the observed data.
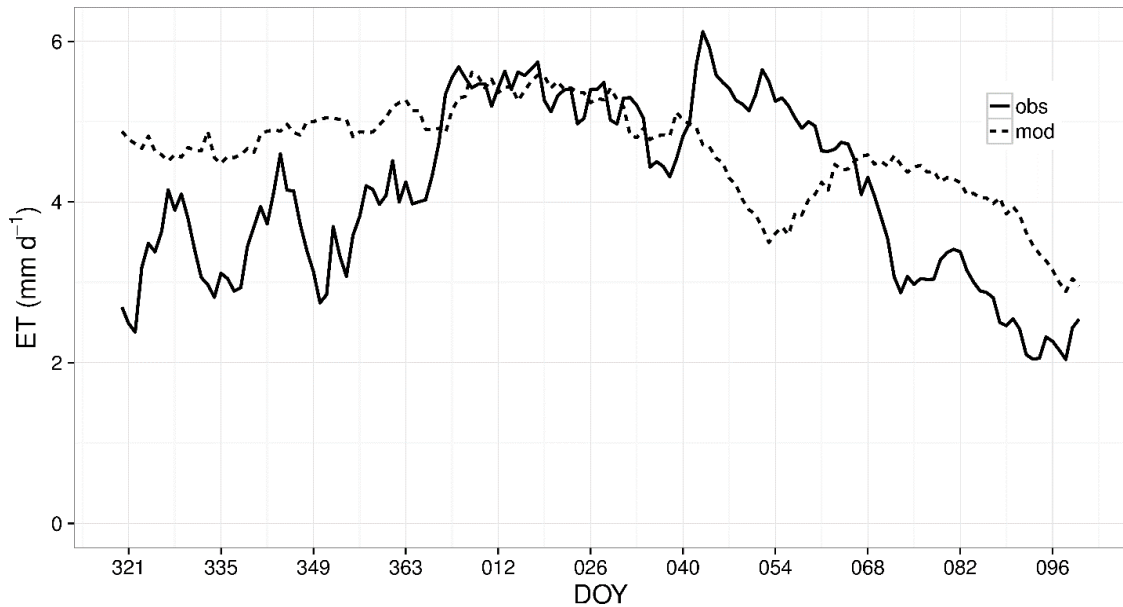
Figure 12. Seasonal cycles of daily evapotranspiration observations at a paddy field in southern Brazil and modeled at the grid closest to the observation site in the 2003/04 growing season.

The contribution of canopy transpiration and soil evaporation to daily ET is shown in Figure 13. Generally, soil evaporation dominates evapotranspiration. However,

during the growing season, when the canopy is dense, canopy transpiration contribution to ET progressively increases until it peaks at 60-70% of ET in the mid-season. Numerous studies based on indirect methods such as the water isotope balance, or model simulations have been done because no direct measurements are available for partitioning evapotranspiration over a paddy field. For example, by coupling land-surface and crop growth models, Maruyama and Kuwagata (2010) suggested that the transpiration contribution to ET was about 45% during the rice growth period. The average transpiration contribution from my results (63%) was higher than that reported in that study. This variability can be attributable to the insufficient consideration and large uncertainty of parameters such as canopy conductance, which were not measured and validated.
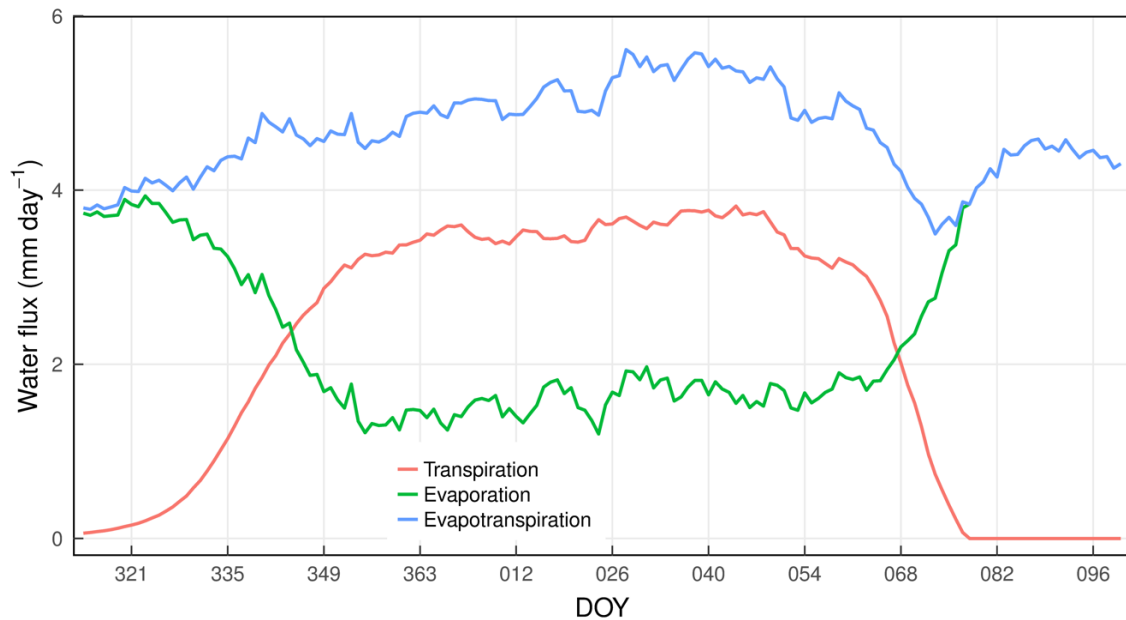
Figure 13. The partitioning of daily evapotranspiration into canopy transpiration and soil evaporation during the 2003/04 growing season.

The daily time series of the modeled water balance components and irrigation during the 2003/04 growing season is illustrated in Figure 14. The irrigation peak shown in the beginning of the crop season (DOY 314) represents the water needed to create the initial standing water in the paddy. Irrigation was applied between DOY 334 and 347 because of low precipitation. During the growing season, total rainfall was 682 mm, total water losses (evaporation, transpiration and drainage) were 1094 mm and total irrigation applied was 915 mm, distributed in 109 days.
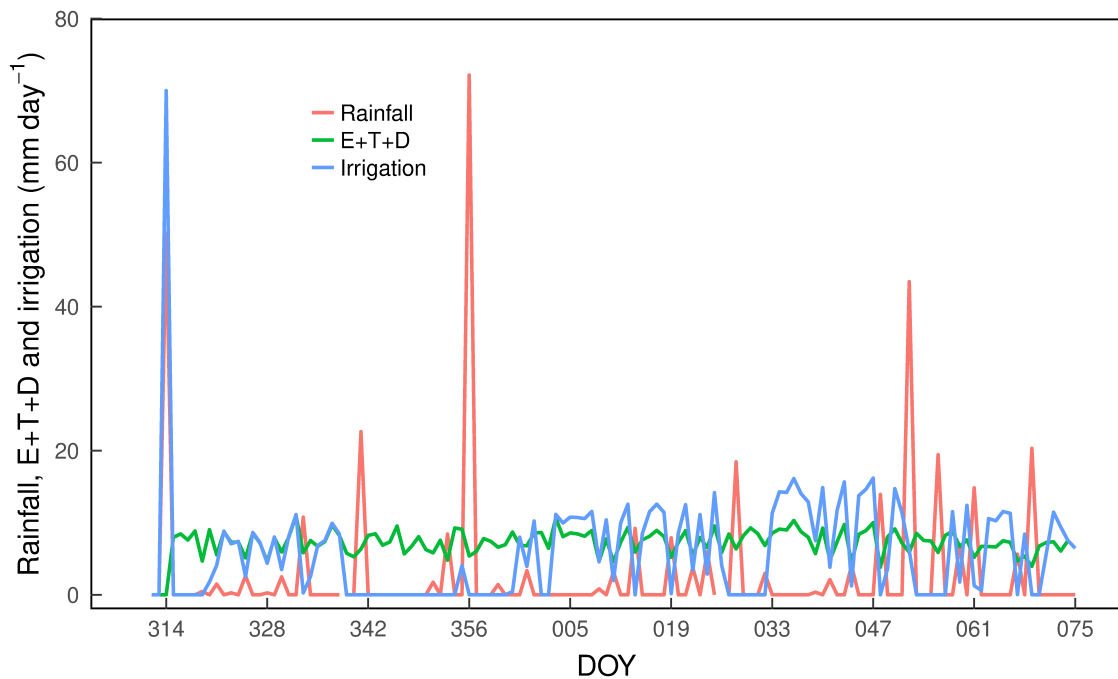
Figure 14. Simulated rainfall, combined evaporation, transpiration and drainage and irrigation during the 2003/04 growing season.

An example of both daily and total seasonal irrigation demand (SID) from Agro-IBIS is illustrated in Figure 15. Relatively low irrigation (around 5 mm) is needed in the beginning of the season and more water (around 15 mm) is applied in the remainder of the growing season. Integrated over the entire growing season, total water applied reaches

46

about 590 mm. Although irrigation data is not available for the study region, these results are found to be consistent with those from Lu et al. (2015), who compared water consumption under four irrigation schedules in northeast China and found that it reached 458 mm in a flooding irrigation plot. These results are also comparable to those by Belder et al. (2004), who reported irrigation input of 415 mm to 588 mm in continuously submerged rice fields in China and the Philippines, respectively.
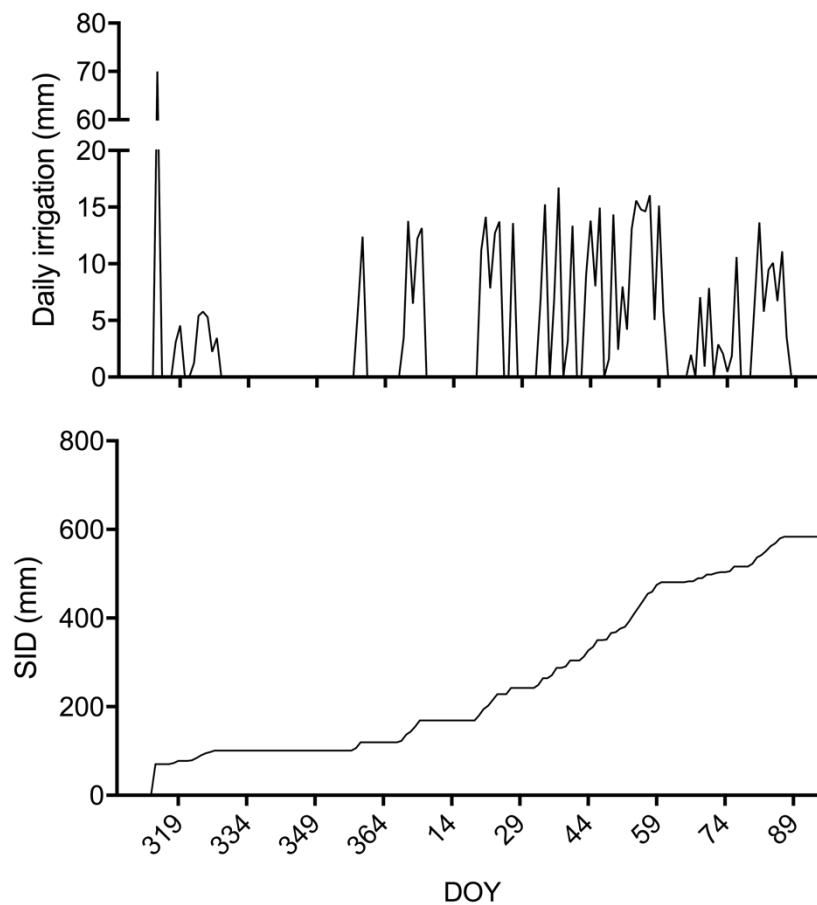
Figure 15. Example of a current climate (1981-2010) simulation of daily irrigation (top) and SID (bottom) at an intensive rice cultivation grid cell in southern Brazil.

Also, personal communication with local extension researchers in southern Brazil reveal that typical irrigation applied over one growing season (~120 days) is

47

approximately 7000 m^3 ha^{-1} of water, which translates to 700 mm per season or on average 5 mm day^{-1}. Finally, according to reports from the International Rice Research Institute (at www.knowledgebank.irri.org/step-by-step-production/growth/water-management), water requirements for lowland rice cultivation can vary from 400 mm to 2000 mm depending on the soil type and the local management practices.

4.2.1   *Regional irrigation in present climate*

The map of the multi-model ensemble mean of present SID in southern Brazil is shown in Figure 16. SID in the study area varies between 167 mm and 520 mm, with an average of 349 mm. The spatial pattern shows that high values (> 400 mm) occur in central and southern RS, in regions characterized by high rice production. Less irrigation (between 300 and 370 mm) is needed in most SC. In northern SC and across most of PR, irrigation is between 250 and 280 mm. In northwestern PR, the most intense rice farming region in the state, irrigation in present climate is less than 200 mm. In general, the simulated irrigation pattern for present climate, including the contrast between the northern and southern portions of the study area, is in agreement with a previous simulation of net irrigation requirements performed by Konzmann et al. (2013). Shahid (2011) found a much higher irrigation demand for rice in northwest Bangladesh, between 840 and 1200 mm, which resulted from a combination of high seepage and percolation losses (280 to 690 mm), high evapotranspiration rates (420 to 480 mm) and exceptionally low rainfall rates (37 to 81 mm).
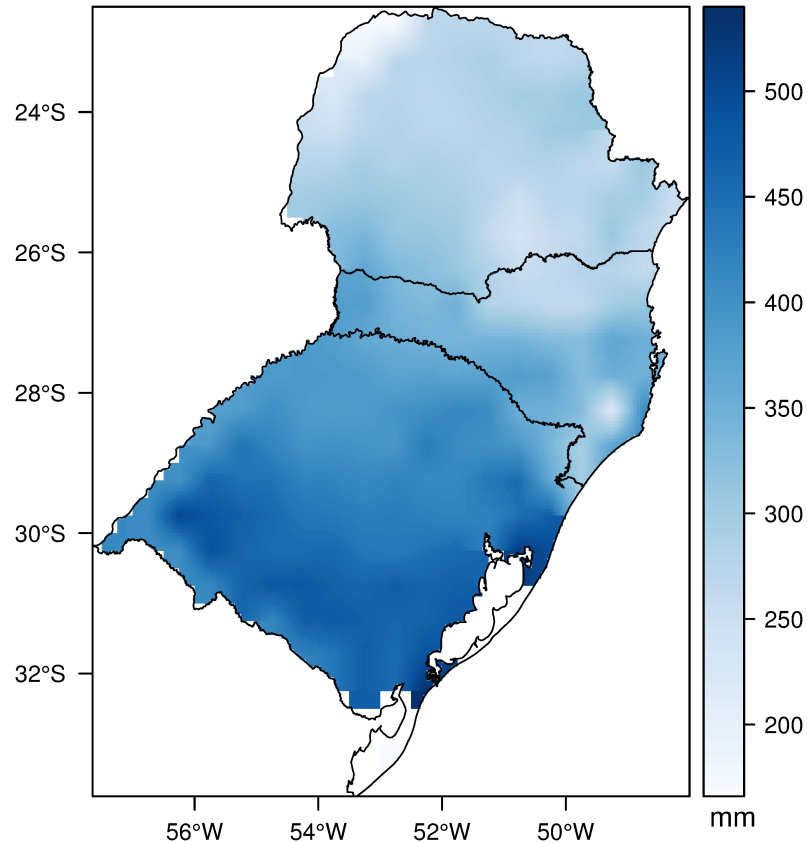
Figure 16. Agro-IBIS simulated map of seasonal irrigation demand for rice irrigation (SID, in mm year^{-1}) in the present climate (1981-2010).

4.3   Rice production under climate change

4.3.1   *Projected changes in temperature during the growing season*

During the period 1981–2010, the mean temperature during the rice-growing period (November–March) presented strong spatial variation and ranged from 19.2°C to 26.6°C in southern Brazil, with the temperatures being highest in the western parts of the study region (Figure 17a) and lowest in the eastern areas between Santa Catarina and Rio Grande do Sul. During the 21st century, temperature is projected to increase generally across the region. In the case of the RCP4.5 emission scenario, the mean temperature from November to March would increase by 0.57°C, 1.1°C and 1.44°C during the periods

2011-40, 2041-2070 and 2071-2100, respectively, relative to the baseline (Figure 17b-d).

In the case of the RCP8.5 emission scenario, the mean temperature from November to

March would increase by 0.66°C, 1.72°C and 2.82°C for the periods 2011-2040, 2041-

2070 and 2071-2100, respectively, relative to the 1981-2010 level, with the largest

increase 3.8°C to 4.0°C in the western part of the study region (Figure 17e-g). These

results are consistent with previous findings by Nuñez et al. (2009) and Marengo et al.

(2010) who reported temperature increases of between 3°C and 5°C for subtropical South

America when analyzing projections from the A2 (Marengo et al., 2010) and A2 and B2

(Nuñez et al., 2009) emission scenarios.
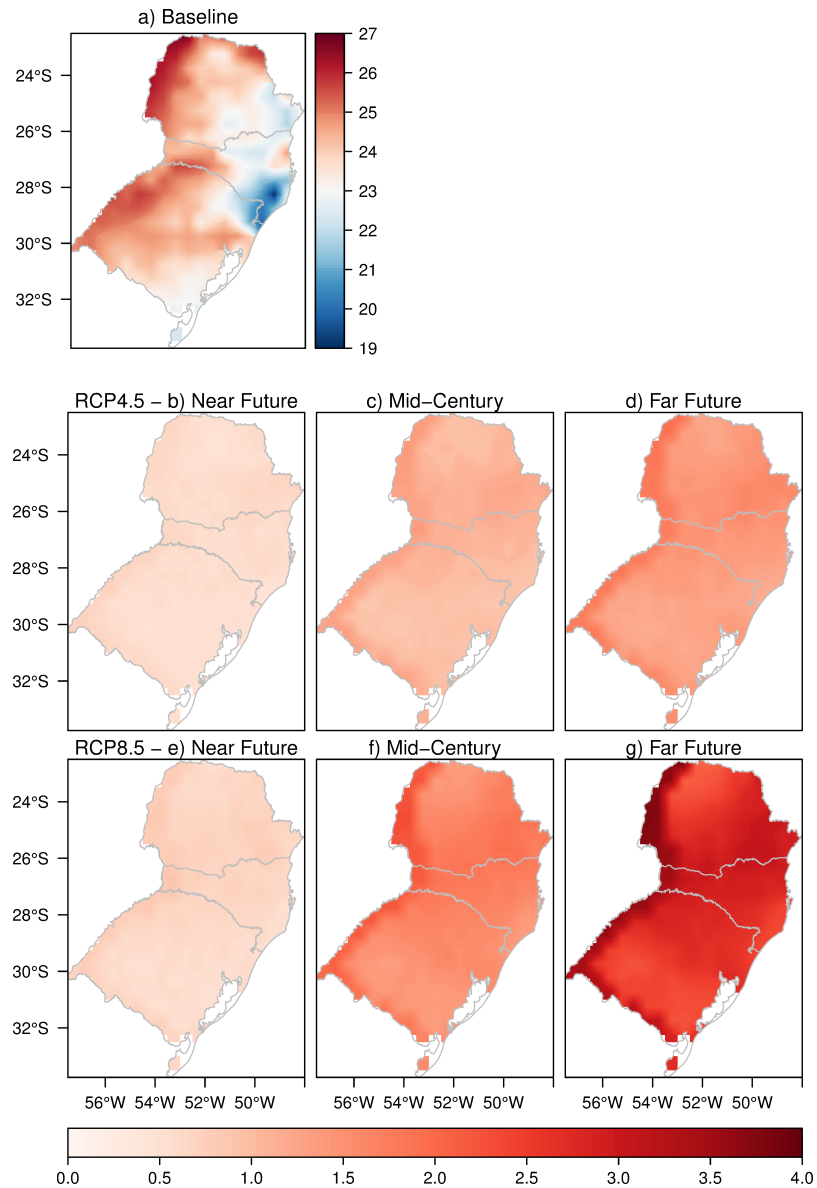
Figure 17. Simulated spatial patterns of mean temperature (°C) during the rice growing season (November to March) for (a) the 1981-2010 baseline period and projected changes in mean temperature (°C) relative to the baseline period for the period 2011-2040 (near future), 2041-2070 (mid-century) and 2071-2100 (far future) under scenarios (b, c and d) RPC4.5 and (e, f and g) RCP8.5.

4.3.2   Projected effects of climate change on rice phenology

Low or high air temperatures extend or reduce the length of rice developmental stages, respectively, and influence the total growing season length. As a result, potential

interruptions in physiological and metabolic processes can cause low yields or even crop

losses. The average simulated changes in the rice growing stages as a response from

rising temperatures from 2011 to 2100 under the RCP4.5 and RCP8.5 scenarios

compared with those under the baseline climate conditions are presented in Figure 18. A

trend of shortening duration was observed in all four growth phases for both the RCP4.5

and RCP8.5 scenarios. On average, under the RCP4.5 scenario the basic vegetative phase

(BVP) would be shortened by one day in the near future and two days in the mid-century

and far future. Under RCP8.5, BVP is projected to be even shorter (by three days) in the

far future relative to the baseline. The photoperiod-sensitive phase (PSP) would advance

three and two days in the near future and mid-century, respectively, both under the RC4.5

and RCP8.5 scenarios. Larger differences were observed in the panicle formation phase

(PFP), which is projected to advance by six to eight days throughout the century,

depending on the emission scenario. The grain-filling phase (GFP) had the same negative

deviation of one day compared to the baseline for all the periods and under both RCP4.5

and RCP8.5 climate scenarios.
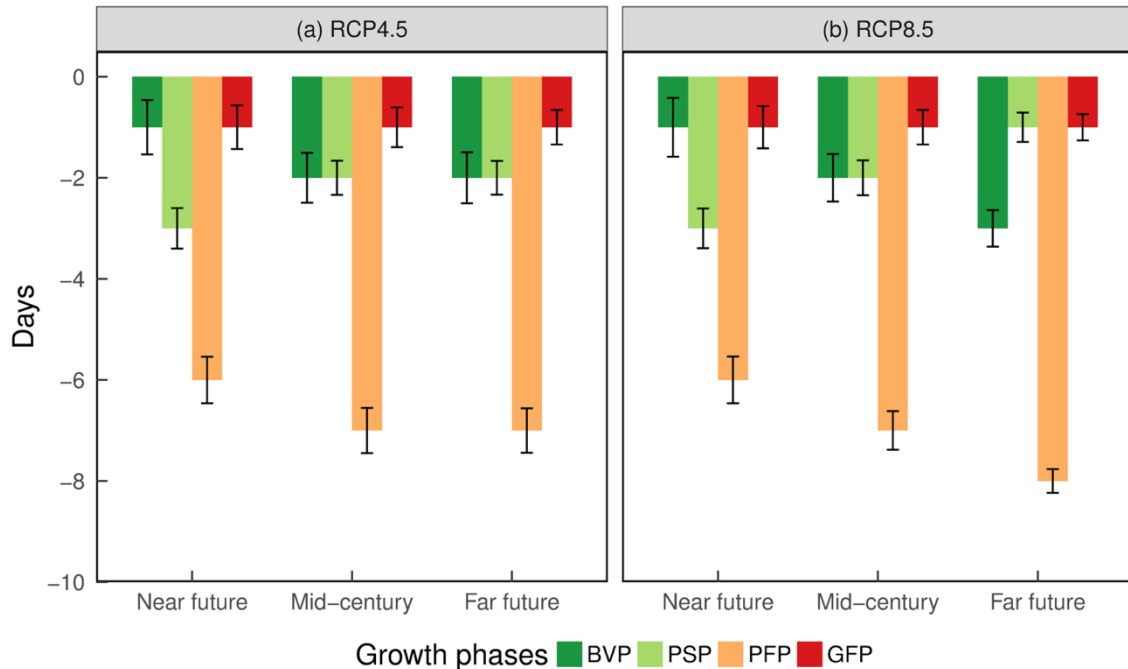
Figure 18. Projected changes in the Agro-IBIS rice growth phases under the future climate scenarios (a) RCP4.5 and (b) RCP8.5. Error bars indicate the standard error of the multi-model ensemble mean.

In addition to changes in the duration of the growth phases, significant changes in rice maturation dates were also found. Under baseline conditions, the modeled date of maturity in rice varied from early March (DOY 65) in the northwestern part of Parana to mid-April (DOY 100) in the eastern portions of the domain (Figure 19a). With the projected climate change, the date of maturity advances for all the domain and under both emission scenarios. On average, under RCP4.5 this change was about three, five and seven days earlier than baseline conditions for the near future, mid-century and far future periods, respectively, whereas under the RCP8.5 scenario the maturation date would be reached on average three, seven and ten days earlier than baseline for the near future, mid-century and far future periods, respectively. The largest changes in rice maturation date, of about 11 days earlier under RCP4.5 (Figure 19b-d) and 20 days earlier under

RCP85 (Figure 19e-g), were seen in the western part of the domain, whereas the smallest changes were found in the eastern part of the domain, where maturity generally occurs later because of cooler conditions during the growing season (Figure 17a).
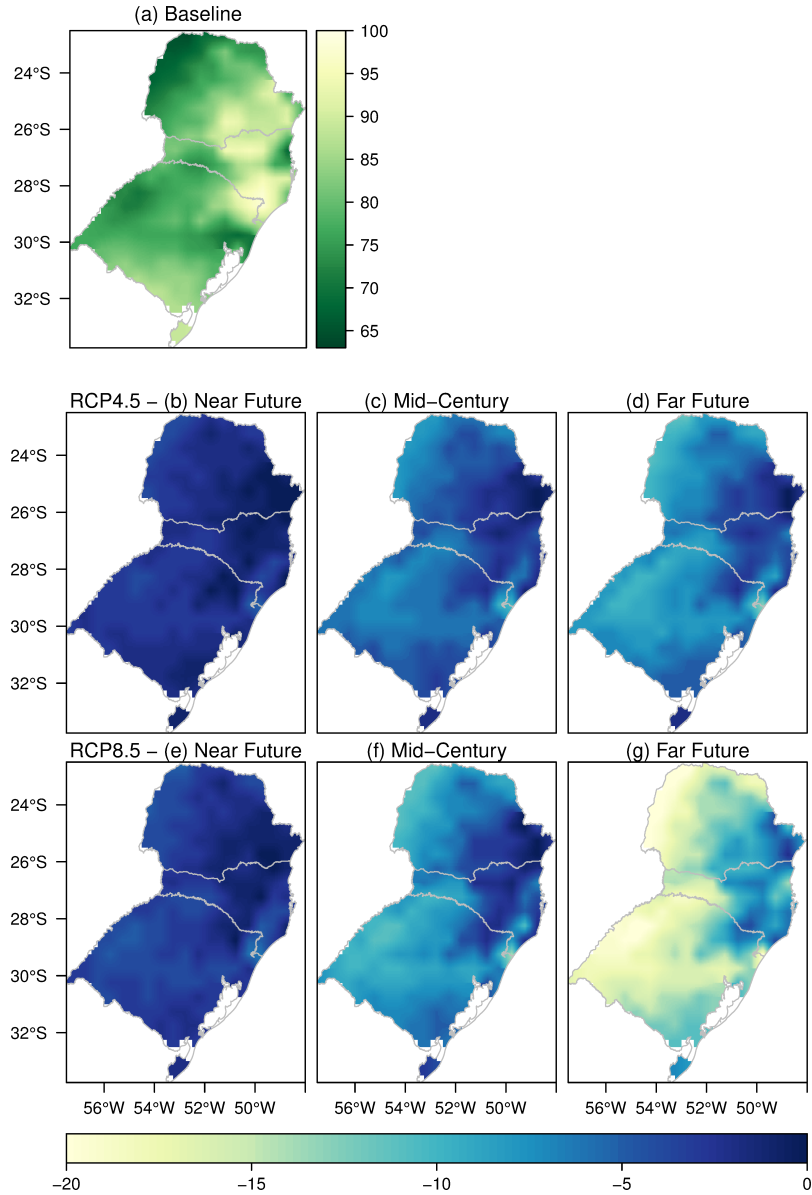
Figure 19. Spatial variations of model-estimated dates of maturity (day of year - DOY) for rice under (a) baseline conditions and projected changes in maturity date (in days) for the period 2011-2040 (near future), 2041-2070 (mid-century) and 2071-2100 (far future) relative to the baseline period (1981-2010) under scenarios (b, c and d) RPC4.5 and (e, f and g) RCP8.5.

This shortening trend is in agreement with, although slightly higher than, previous studies which have shown that rice crop phenology will be advanced and the growth window could be lengthened in the future as a result of climatic warming (Prasad et al., 2006; Tao, Yokozawa, Xu, Hayashi, & Zhang, 2006; Zhang, Huang, & Yang, 2013). Although all four rice growth stages considered in this study were projected to shorten, the least impacted was the grain-filling phase (GFP). It was previously suggested that prolonged exposure to temperatures above 25°C causes a yield decline in rice due to shorter grain filling duration (Chowdhury & Wardlaw, 1978; Hatfield & Prueger, 2015). However, since GFP would be shortened by only one day in our simulations, it is unlikely that the direct effect of the hastened growth duration would have a large impact on the rice yield (see next section).

4.3.3 *Projected effects of climate change on rice yields*

When the CO_2 fertilization effect was not taken into account, it was found that average yields across southern Brazil are likely to decrease by 3-12% and by 4-30% under the RCP4.5 and RCP8.5 emission scenarios, respectively (Table 7). On the other hand, average yields across the study region are projected to increase by 13-23% and 14-35% under the RCP4.5 and RCP8.5 emission scenarios, respectively, when the direct effect of CO_2 fertilization is included in the simulations. Note, however, the large regional variability in the yield changes (Figure 20 and Figure 21).

Table 7. Mean projected changes (%) in southern Brazil's rice yield compared with baseline's yield (1981-2010). The range represents the standard error of the multi-model ensemble mean.

Period	Without CO_2 fertilization		With CO_2 fertilization	
	RCP4.5	RCP8.5	RCP4.5	RCP8.5
Near future	-3.1 (±1.5)	-3.8 (±1.5)	12.8 (±1.3)	14.0 (±1.5)
Mid-century	-7.8 (±2.8)	-15.0 (±3.7)	21.6 (±2.3)	26.3 (±2.9)
Far future	-12.1 (±3.6)	-29.7 (±6.8)	23.4 (±2.5)	35.1 (±5.4)

The spatial patterns of simulated changes in rice yields relative to the baseline during the near future (2011-2040), mid-century (2041-2070) and far future (2071-2100) periods, if CO_2 fertilization effects are not taken into account, are presented in Figure 20. In both RCP4.5 and RCP8.5 climates, rice yield in the productive areas across most of the study region are projected to decrease relative to the 1981-2010 baseline period. In contrast, in areas of northeastern Rio Grande do Sul and southeastern Santa Catarina with lower mean temperature during 1981-2010 (Figure 17a), rice yields were projected to increase by up to 61% under RCP4.5 and 85% under RCP8.5 by the end of the century (Figure 20).
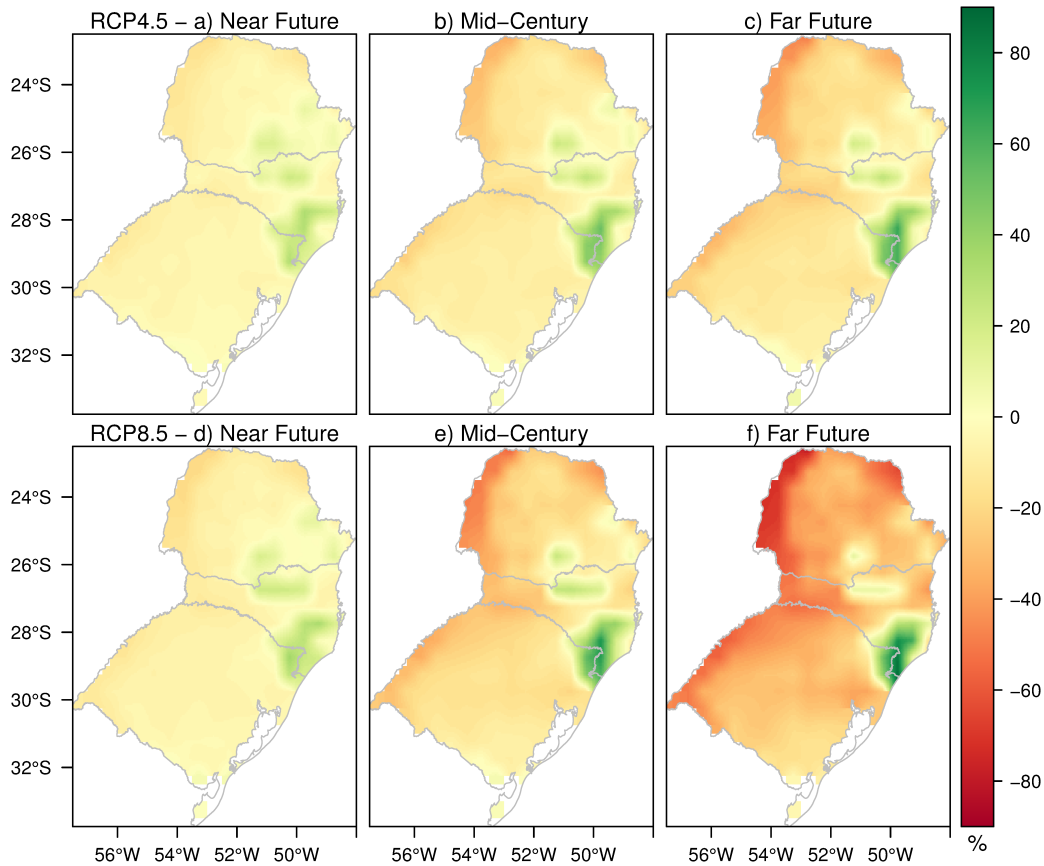
Figure 20. Projected spatial variations of changes in rice yield for the periods 2011-2040 (near future), 2041-2070 (mid-century) and 2071-2100 (far future) in comparison to 1981–2010 baseline without CO_2 fertilization effects under scenarios RCP4.5 (a, b and c) and RCP8.5 (d, e and f).

The spatial patterns of simulated changes in rice yields when CO_2 fertilization effects are included are presented in Figure 21. The simulations show that the effect of elevated CO_2 alleviates yield losses in the whole study region. When taking CO_2 fertilization effects into account, it was found that rice yield increases over most of southern Brazil, generally by 5-30% throughout the 21st century under RCP4.5 (Figure 21a-c) and by 9-39% under RCP8.5 (Figure 21d-f). Yield responses to elevated CO_2 were more prominent in southeastern Santa Catarina, where mean growing-season temperatures under baseline conditions were lower, but also in northern Paraná where

growing-season temperatures in baseline were higher, thus suggesting that the negative

impact on yield caused by high temperature was compensated by the CO_2 fertilization
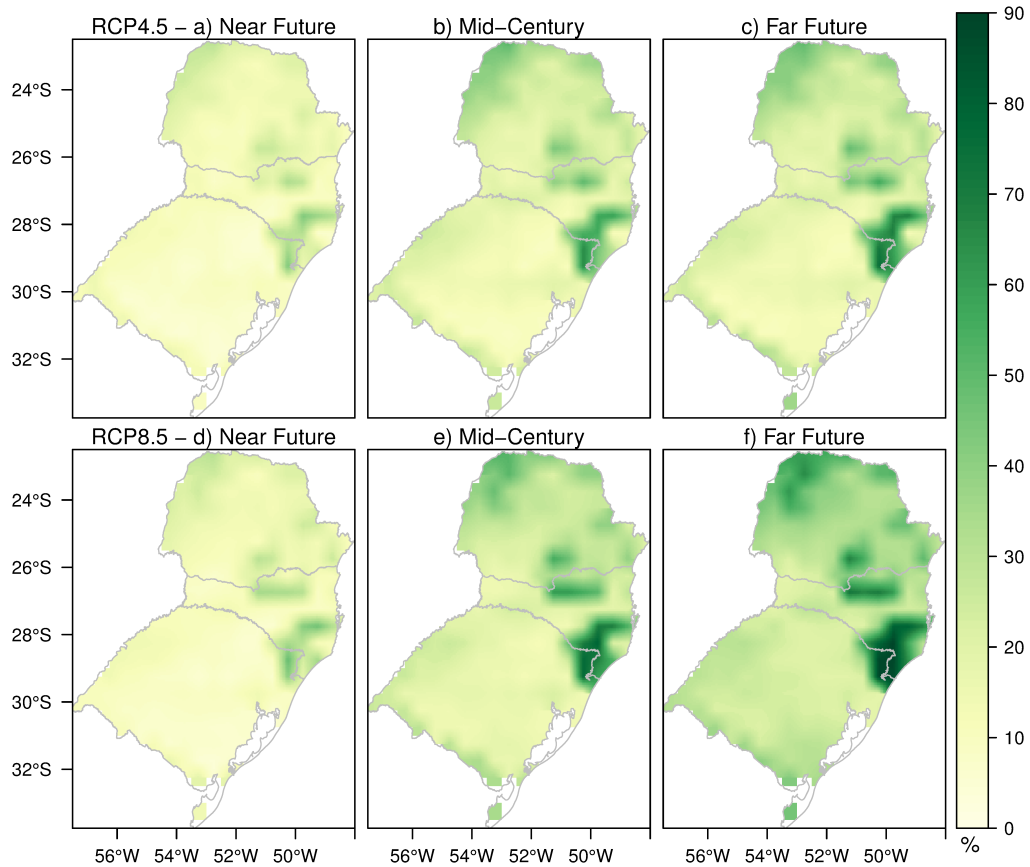
effect.

Figure 21. As in Figure 20, but with consideration of CO_2 fertilization effects.

The results show that the patterns of change in yield, in both the STA-CO_2 and

DYN-CO_2 experiments (Figure 20 and Figure 21), as well as the change in duration of

the rice-growing period (Figure 19), were spatially coherent with the pattern of

temperature, suggesting temperature and its change are projected to play a significant role

in affecting rice yield in southern Brazil. In general, our results are consistent with

findings from previous field studies (B. A. Kimball et al., 2002; Vu et al., 1997) and

modeling studies as well (Deryng, Conway, Ramankutty, Price, & Warren, 2014; Erda et al., 2005).

Based on the STA-CO$_2$ simulations, it was found that even the smallest predicted higher temperatures due to climate change will reduce yields in most of southern Brazil. Hence, most of the rice planting areas in southern Brazil appear to be already at optimum temperatures. The only exception seems to be the productive region in southeastern SC/northeastern RS, where temperatures are currently at suboptimum, and therefore is projected to benefit by higher temperatures alone and/or by combined increasing temperature and CO$_2$ concentration.

4.4   Rice irrigation under climate change

Besides the direct impacts of climate change on crop production, there is also concern about increasing future agricultural water requirements caused by the combined effects of climate change (i.e. rising temperature and irregularly distributed rainfall). In this section I present the projected changes in rice irrigation water requirements in southern Brazil throughout the 21st century. Table 8 summarizes the multi-model ensemble mean values of SID in the different periods in the three states of the study region. These results are reported for the region of study by using simple area averages over the domain for all simulated periods, from November to March. Average SID showed a decreasing tendency in PR for the two scenarios. Average SID in SC was 4.6% (near future), 7.6% (mid-century) and 4.7% (far future) higher than the baseline under RCP4.5 and 3.3% (near future), 5.2% (mid-century) and 1.9% (far future) higher than baseline under RCP8.5.

Table 8. Relative difference of projected SID (in mm) between future scenarios and the baseline (1981-2010) in each state of southern Brazil for the period 2011-2100. As a reference, average SID in present climate is 274.9 mm in PR, 317.7 mm in SC, 416.4 mm in RS (348.9 mm in the entire region).

| State | Future | RCP4.5 | | RCP8.5 | |
		Mean (mm)	Δ present (%)	Mean (mm)	Δ present (%)
	Near	274.13	-0.3	268.05	-2.5
PR	Mid	266.87	-2.9	252.64	-8.1
	Far	262.64	-4.5	234.59	-14.7
	Near	332.31	4.6	328.05	3.3
SC	Mid	341.79	7.6	334.28	5.2
	Far	332.79	4.7	323.91	1.9
	Near	424.91	2.0	421.62	1.2
RS	Mid	431.72	3.7	417.71	0.3
	Far	418.76	0.6	395.09	-5.1
	Near	355.18	1.8	350.74	0.5
Regional	Mid	357.51	2.5	344.58	-1.2
	Far	348.34	-0.2	325.76	-6.6

The spatial variation of SID in southern Brazil during the growing season (November to March) throughout the twenty-first century, relative to present climate, is shown in Figure 22. As a result of projected future climate conditions, SID exhibits variable spatial distribution for both climate scenarios. Under RCP4.5, SID decreases slightly (<10%) in most of PR in the near future. Through mid-century and far future, SID decreases between 10% and 20% in most of PR but slight increased SID (<10%) is observed in southeastern PR from mid-century onwards. Under RCP8.5, SID in western and northern PR is projected to decrease around 30% in the mid-century and 40% by the end of the century. Under the RCP4.5 climate scenario, rice fields in southeastern (eastern) SC are projected to demand around 20% more (8% less) irrigation than the present. Under RCP8.5, SID is projected to increase around 40% in southeast SC relative to present climate. Simulation results for RS indicate that the rice fields in the center of

the state might require less irrigation, whereas the southernmost portion of the state might

require more water use.
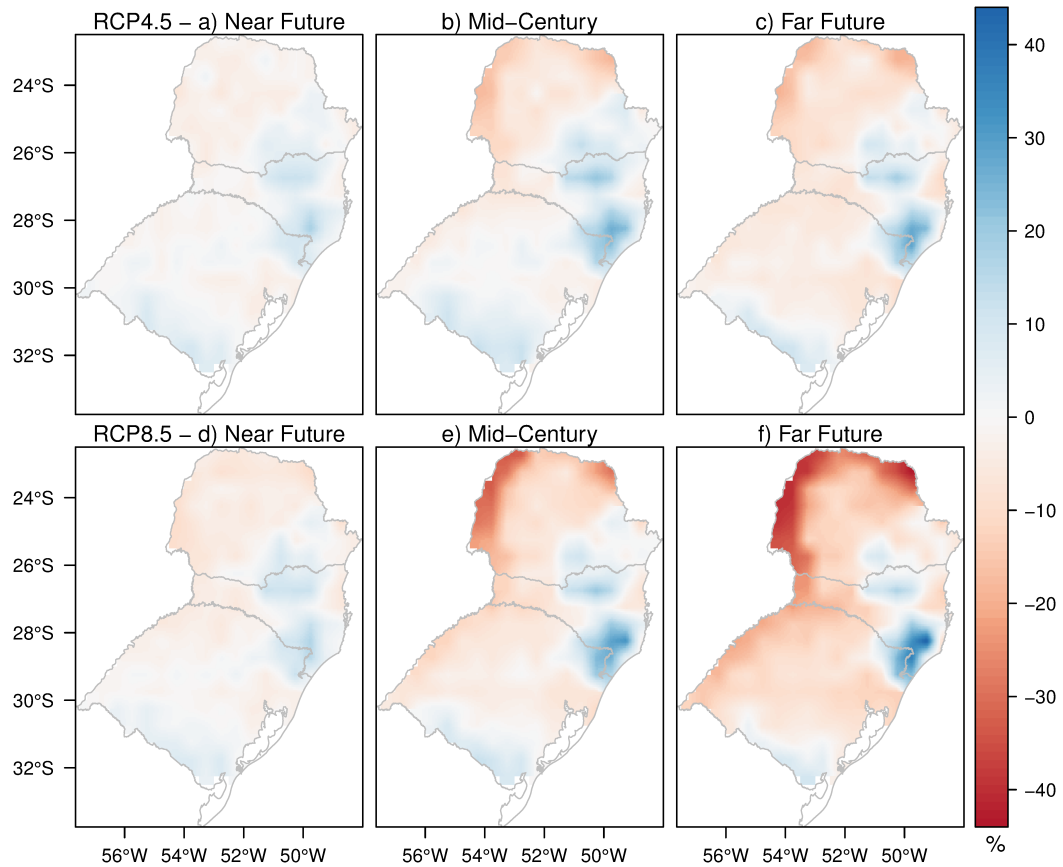
Figure 22. Spatial pattern of relative change (%) of SID throughout the twentieth century
(2011-2100) under emission scenarios RCP4.5 (a, b and c) and RCP8.5 (d ,e and f)
compared to the present climate (1981-2010).

4.4.1   Changes in water balance

To understand the impact of projected climate changes on SID, changes in rainfall

and evapotranspiration (combined evaporation and transpiration from Agro-IBIS) in

future climate relative to the baseline are summarized. On average, the seasonal rainfall

for southern Brazil was 1019.6 mm for the baseline period and is projected to increase in

all three states in the region (Table 9). In current climate, the largest rainfall observed is 1039.4 mm in PR and the smallest rainfall is 976.7 mm for RS.

Table 9. Relative difference of projected rainfall (in mm) between future scenarios and the baseline (1981-2010) in each state of southern Brazil for the period 2011-2100. As a reference, average rainfall in present climate is 1039.9 mm in PR, 1091.2 mm in SC and 976.7 mm in RS (1019.6 mm for the entire region).

State	Future	RCP4.5		RCP8.5	
		Mean (mm)	Δ present (%)	Mean (mm)	Δ present (%)
PR	Near	1079.56	3.8	1080.91	3.9
	Mid	1093.68	5.2	1093.76	5.2
	Far	1095.20	5.3	1119.61	7.7
SC	Near	1132.93	3.8	1142.97	4.7
	Mid	1155.82	5.9	1172.23	7.4
	Far	1173.11	7.5	1213.01	11.2
RS	Near	1009.75	3.4	1021.69	4.6
	Mid	1034.79	5.9	1056.19	8.1
	Far	1052.89	7.8	1085.43	11.1
Regional	Near	1056.39	3.6	1064.25	4.4
	Mid	1077.19	5.6	1090.18	6.9
	Far	1089.30	6.8	1120.29	9.9

The average rainfall of the entire region was 1056.4 mm (near future), 1077.2 mm (mid-century) and 1089.3 mm (far future) under the RCP4.5 scenario, and these were respectively 3.6% and 5.6% and 6.8% larger than those of the baseline. Under RCP8.5, seasonal rainfall for the entire region increased to 1064.2 mm (near future), 1090.2 mm (mid-century) and 1120.3 mm (far future), which represents increases of respectively 4.4%, 6.9% and 9.9% from the baseline.

Table 10 shows the simulated evapotranspiration during the growing season for the baseline and future scenarios in the major rice-growing areas in each of the three

states. Average ET for southern Brazil is 756.4 mm for the baseline, and it showed an

increasing tendency across the region over the 21st century.

Table 10. Relative difference of projected evapotranspiration (ET, in mm) between future scenarios and the baseline (1981-2010) in each state of southern Brazil for the period 2011-2100. As a reference, ET in present climate (1981-2010) is 726.7 mm in PR, 780.1 mm in SC and 769.8 mm in RS (756.4 mm for the entire region).

State	Future	RCP4.5		RCP8.5	
		Mean (mm)	Δ present (%)	Mean (mm)	Δ present (%)
	Near	751.60	3.4	746.90	2.8
PR	Mid	766.65	5.5	776.97	6.9
	Far	774.42	6.6	794.57	9.3
	Near	805.95	3.3	804.51	3.1
SC	Mid	829.37	6.3	841.68	7.9
	Far	832.20	6.7	866.38	11.1
	Near	799.03	3.8	797.32	3.6
RS	Mid	819.19	6.4	830.02	7.8
	Far	823.63	7.0	847.51	10.1
	Near	783.54	3.6	780.82	3.2
Regional	Mid	802.48	6.1	813.40	7.5
	Far	807.81	6.8	832.22	10.1

Although no moisture deficit (precipitation minus ET) is observed by the end of the

growing season (Table 9 and Table 10), how can SID be negative in some areas? It is

speculated that cumulative values over the growing season do not capture the daily

variation of the balance between precipitation and evapotranspiration that drives the need

for irrigation. Therefore, the difference between irrigation days in future and present

climate is shown. "Irrigation days" are defined as the number of days during the growing

season when irrigation applied was greater than 0 mm. The ensemble-mean changes in

irrigation days (future minus present climate) in response to anthropogenic forcing are

shown in Table 11. Over PR the number of irrigation days may decline by about 1 (near

future), 2 (mid-century) and 3 days (far future) under RCP4.5 and by about 2 (near

future), 5 (mid-century) and 7 days (far future) under RCP8.5.

Table 11. Absolute difference in projected irrigation days between future scenarios and
the baseline (1981-2010) in each state of southern Brazil for the period 2011-2100.

State	Future	RCP4.5		RCP8.5	
		Mean (days)	Δ present (days)	Mean (days)	Δ present (days)
	Near	37	-1	36	-2
PR	Mid	36	-2	34	-5
	Far	35	-3	31	-7
	Near	43	1	43	1
SC	Mid	44	3	43	2
	Far	43	1	41	1
	Near	56	1	55	1
RS	Mid	55	2	54	0
	Far	54	0	50	-3
	Near	47	0	46	0
Regional	Mid	47	0	45	-2
	Far	45	-2	42	-5

On average, irrigation days may increase in SC in both scenarios, ranging from one (near

future), three (mid-century) and one (far future) days under RCP4.5 and one (near future),

two (mid-century) and one (far future) days under RCP8.5. RS might experience more or

less irrigation days, depending on the scenario. Under RCP4.5, irrigation days will be

shortened by one and two days in the near future and mid-century, with no changes

projected for the end of the century. Under RCP8.5, however, irrigation days over the

season are projected to increase by one day in the near future and decrease by three days

by the end of the century.

4.4.2 Water consumption in future climates

Calculating the total irrigation demand (as volume), rather than average irrigation requirements (as depth), helps to more realistically represent water consumption by taking into account only areas where rice is grown. When the cell value of the net SID (Figure 16) is multiplied by the fraction of each 0.5° by 0.5° cell area (m^2) where rice is harvested in each state (Figure 1b), the volumetric water demand (VWD, in m^3) is obtained (Table 12). These values represent the total volume of water required over a certain region and can be directly compared with, for example, river discharge or water stored in reservoirs.

These calculations were made under the assumption that rice productive areas in southern Brazil will have the same spatial distribution in the future as in the present. VWD for current climate was estimated as 193 Mm^3 yr^{-1} in PR, 614 Mm^3 yr^{-1} in SC, 3992 Mm^3 yr^{-1} in RS and a combined 4798 Mm^3 yr^{-1} for southern Brazil. This value is comparable to, although lower than, the 7396 Mm^3 yr^{-1} that Chapagain and Hoekstra (2011) found for blue irrigation (the consumption of blue water resources - surface and ground water) in Brazil. However, their estimation was under assumptions slightly different than those used in this study. For example, they assume the use of a 200 mm water layer to saturate the soil prior to planting, where this study consider 70 mm. Also, they consider a permanent water layer of 100 mm during the season, while this study assume a minimum of 30 mm.

A comparison between VWD for rice irrigation in present and future climate is reported in Table 12. On average for the region, total future volumes of water required to grow rice were projected to increase in most cases, by 1.8% (near future RCP4.5), 3.6%

(mid-century RCP4.5) and 1.2% (far future RCP4.5). Under RCP8.5, regional

consumption is projected to increase 1.3% in the near future, 0.6% in mid-century, but is

projected to decrease by 3.5% in the far future. In PR, under a medium-emission climate

scenario, water consumption is projected to reduce by 0.3%, 3.9% and 5.4% in the near

future, mid-century and far future respectively, compared to present climate. Under a

high-emission scenario, volumes are projected to decrease by 2.6% (near future), 9.1%

(mid-century) and 15.7% (far future). The largest increase in VWD occurs in SC, where

irrigation is projected to increase by 3.2% (near future), 9.3% (mid-century) and 7.6%

(far future) under the RCP4.5 scenario and 3.5% (near future), 8.6% (mid-century) and

9.4% (far future) under the RCP8.5 scenario.

Table 12. Relative difference of projected VWD (in Mm^3 yr^{-1}) between future scenarios and the baseline (1981-2010) in the rice productive regions in each state of southern Brazil. As a reference, VWD in present climate is 193 Mm^3 yr^{-1} in PR, 614 Mm^3 yr^{-1} in SC and 3992 Mm^3 yr^{-1} in RS (4798 Mm^3 yr^{-1} for the entire region).

State	Future	RCP4.5		RCP8.5	
		Mean (Mm^3)	Δ present (%)	Mean (Mm^3)	Δ present (%)
	Near	192.82	-0.3	188.42	-2.6
PR	Mid	186.00	-3.9	175.82	-9.1
	Far	182.95	-5.4	163.06	-15.7
	Near	633.48	3.2	634.98	3.5
SC	Mid	670.42	9.3	666.47	8.6
	Far	660.50	7.6	671.32	9.4
	Near	4061.14	1.7	4040.19	1.2
RS	Mid	4116.36	3.1	3983.43	-0.2
	Far	4015.11	0.6	3796.75	-4.9
	Near	4887.44	1.8	4863.59	1.3
Regional	Mid	4972.78	3.6	4825.71	0.6
	Far	4858.56	1.2	4631.14	-3.5

In RS, VWD in the near-future is projected to increase in both scenarios, but it can either increase or decrease in the mid-century and far future, depending on the climate scenario. Our results are in agreement with those reported by Chung et al. (2011), who found higher future volumetric irrigation demand in South Korea, in comparison to the baseline period of 1971-2000.

Chapter 5. General conclusions and recommendations

In this dissertation a new process-based rice growth model was developed and integrated into the dynamic ecosystem model Agro-IBIS. The updated Agro-IBIS has two features: (i) the model can simulate leaf area index (LAI), biomass growth for each carbon pool (leaves, stems and reproductive organs) and crop yield by taking into account a phenological stage indicator that is sensitive to both heat accumulation and photoperiod during the growing season; (ii) the model considers water surface and irrigation in paddy rice fields.

The comparison of LAI , biomass and duration of phases of development between simulations and observations at the validation sites in Brazil and Philippines showed that Agro-IBIS's predictions were in good agreement with the observations. Based on experimentally-derived growth rates of four key growth stages of rice, the model showed a tendency of overestimating the duration of the every growth stage in two growing seasons in southern Brazil. This might be an indicative of a cold bias in the climate data used to run the model. Predictions of LAI and biomass showed a good temporal coherence with observations, and the cumulative end of season errors were not higher than 11%.

The comparison between simulated evapotranspiration (ET) and micrometeorological measurements in southern Brazil showed that Agro-IBIS tends to overestimate ET in the early growing season weeks and underestimate ET in the late weeks, but showed a cumulative end of season ET error of 9%. A realistic representation of cumulative end-of-season ET is important because the rice irrigation model is based on

the water balance approach, which keeps track of the surface water deficit by accounting for all water additions and subtractions from the surface water layer of the paddy field.

To project possible changes in rice productivity and water use in southern Brazil due to future climate change, the output from five climate models of the Coupled Model Intercomparison Project Phase 5 (CMIP5), under the two emission scenarios RCP4.5 and RCP8.5, excluding and including CO_2 fertilization effects, were used to run Agro-IBIS from the period 2011 to 2100 and compared to the baseline period from 1981-2010.

The simulations showed that the higher temperatures projected for southern Brazil throughout the 21st century can significantly advance rice phenology by up to 20 days, but on average by 11 days. In the simulations excluding the CO_2 fertilization effect, higher-than-optimum temperatures played an important role in reducing rice yields in most of the region relative to 1981-2010. When CO_2 fertilization was taken into account, photosynthetic stimulation induced by rising CO_2 concentrations could exceed the negative effect of increased temperature on rice growth, thus contributing to higher yields throughout the 21 century relative to the baseline period 1981-2010. Although maturity was projected to advance significantly, yield was not affected because the advancement was smaller during grain filling.

I also analyzed the projected impact of climatic changes on paddy irrigation requirements and volumetric irrigation water demands with respect to the reference period 1981–2010. The primary conclusions can be summarized as follows: across southern Brazil, the growing season rainfall amounts for the future scenarios were projected to increase on average by 3.6–10%. Evaporation and transpiration were also projected to increase, but not enough to create a net moisture deficit by the end of the

growing season. As a consequence, the number of irrigation days in the season is projected to reduce by up to five days.

The spatial variations of seasonal irrigation demand (SID) for rice in southern Brazil are large and their projected variations compared to present climate varied from -40% to 40%, depending on the state and the emission scenario. Farmers from northern Parana and most of Rio Grande do Sul might benefit economically from lower climatic irrigation requirements. In contrast, farmers in eastern Santa Catarina and northeastern Rio Grande do Sul might have to adapt to grow rice under greater water demand. Other studies examined consequences to Brazilian agriculture caused by potential climate constraints. For example, a southward latitudinal migration of Arabica coffee was proposed by Zullo et al. (2011) as a consequence of projected warming of +2°C to +3°C in a regional study in Brazil.

The spatial and temporal variations of irrigation demand for the future should be taken into account in future irrigation planning and management. Installing irrigation in new fields is expensive, and producers will only install irrigation if they find the increased revenue from crops grown on irrigated fields worth more than the cost of irrigation. Brazil is a developing country facing the challenges of climate change, while also pursuing sustainable economic development. Consequently, any economic feasibility of climate change mitigation measures has great importance.

Although the results suggest that less irrigation would potentially save water and provide economic benefits for Rio Grande do Sul, more rain in a changing climate can also be associated with more extreme events. Excessive rainfall during the planting season or early growing stages could cause delays in plant development, creating a risk for both

productivity and profitability of crops (Rosenzweig, Tubiello, Goldberg, Mills, & Bloomfield, 2002). Crop losses associated with anoxia, increased susceptibility to diseases and more runoff and leaching of nutrients and chemicals into ground and surface waters may also occur as the result of excessive soil water. Also, higher volumetric irrigation would require additional water withdrawals from reservoirs, lakes and rivers which can also pose environmental problems. However, further research would be required to investigate these issues focusing on rice production in southern Brazil.

It is worth mentioning some limitations of this research that could be addressed in future studies. First, despite the simplicity advantage of the quantile-mapping method in generating bias-free climate data that preserve the characteristics of observed monthly weather events, like all statistical downscaling approaches it assumes that biases associated to historical observations will be constant in the projection period. While this might hold true for shorter periods of time, statistical bias-removal methods are unable to account for the nonlinear interactions between climate variables over longer periods. It is possible to overcome this limitation by using dynamically downscaled data from a regional climate model forced with data from general circulation models. For example, the Coordinated Regional Climate Downscaling Experiment (CORDEX - Giorgi et al., 2009) was created by the World Climate Research Program to provide downscaled climate output for all continents. It would be worth exploring the potential of the CORDEX dataset in future simulations using Agro-IBIS over South America.

Consequently, it is worth acknowledging that the estimated impacts of climate changes examined in this study should not be interpreted as representing the correct, expected climate change impacts. Rather, the results are meant to provide a measure of

the sensitivity of rice yields to changes in temperature, rainfall and CO_2 concentration in southern Brazil, a relevant rice-producer area that has received little attention. Rice is one of the major staple crops consumed worldwide, and in Brazil an estimated 60% of the population consumes the grain daily. Basic self-sufficiency of the rice supply in the future will be of fundamental importance not only for food and economic security in Brazil but also for the sustainability of the world's food market.

Rice, like any other C_3 plant, benefits from elevated atmospheric CO_2 by accelerating photosynthesis rates on its leaves via both enrichment of substrate CO_2 and inhibition of photorespiration due to a higher CO_2 concentration. However, photosynthetic rates of leaves exposed to higher CO_2 concentration are generally lower than those of leaves that have been kept in ambient CO_2 concentration, which is referred to as CO_2 acclimation. The current Agro-IBIS rice parameterization is unable to represent such an acclimation process, which has the potential to cause an overestimation of the yield responses to increased CO_2. For example, Twine et al. (2013) used maximum carboxylation rate of photosynthesis (V_{max}) values of 40.53 and 37.4 μmol CO_2 m^2 s^{-1} to simulate Agro-IBIS' soybean responses to ambient (375 ppm) and elevated (550 ppm) CO_2 concentrations, respectively. By making this adjustment, they found more realistic responses of soybean yield to elevated CO_2 concentration when compared to soybean FACE observations . In future runs using Agro-IBIS rice, refinements in the V_{max} parameter are recommended to account for CO_2 acclimation.

BIBLIOGRAPHY

Ainsworth, E. A. (2008). Rice production in a changing climate: A meta-analysis of responses to elevated carbon dioxide and elevated ozone concentration. *Global Change Biology*, *14*(7), 1642–1650. https://doi.org/10.1111/j.1365-2486.2008.01594.x

Ainsworth, E. A., & Long, S. P. (2005). What have we learned from 15 years of free-air CO2 enrichment (FACE)? A meta-analytic review of the responses of photosynthesis, canopy properties and plant production to rising CO2. *New Phytologist*, *165*(2), 351–372. https://doi.org/10.1111/j.1469-8137.2004.01224.x

Alexandratos, N., & Bruinsma, J. (2012). *World agriculture towards 2030/2050: the 2012 revision*. *ESA Working Paper* (Vol. 12). https://doi.org/10.1016/S0264-8377(03)00047-4

Anbumozhi, V., Yamaji, E., & Tabuchi, T. (1998). Rice crop growth and yield as influenced by changes in ponding water depth, water regime and fertigation level. *Agricultural Water Management*, *37*(3), 241–253. https://doi.org/10.1016/S0378-3774(98)00041-9

Asch, F., Sow, A., & Dingkuhn, M. (1999). Reserve mobilization , dry matter partitioning and specific leaf area in seedlings of African rice cultivars differing in early vigor. *Fields Crop Research*, *62*, 191–202.

Baker, J. T., Allen, L. H., & Boote, K. J. (1990). Growth and yield responses of rice to carbon dioxide concentration. *The Journal of Agricultural Science*, *115*(9863), 313. https://doi.org/10.1017/S0021859600075729

Baker, J. T., Allen, L. H., & Boote, K. J. (1992). Response of rice to carbon dioxide and

temperature. *Agricultural and Forest Meteorology*, *60*(3–4), 153–166.

https://doi.org/10.1016/0168-1923(92)90035-3

Baker, J. T., Allen, L. H., Boote, K. J., Jones, P., & Jones, J. W. (1990). Rice

Photosynthesis and Evapotranspiration in Subambient, Ambient, and Superambient

Carbon Dioxide Concentrations. *Agronomy Journal*, *82*(4), 834.

https://doi.org/10.2134/agronj1990.00021962008200040034x

Baker, J. T., & Allen, L. H. J. (1993). Effects of CO2 and temperature on rice: a summary

of five growing seasons. *Journal of Agricultural Meteorology*, *48*(5), 575–582.

Belder, P., Bouman, B. A. M., Cabangon, R., Guoan, L., Quilang, E. J. P., Yuanhua, L.,

… Tuong, T. P. (2004). Effect of water-saving irrigation on rice yield and water use

in typical lowland conditions in Asia. *Agricultural Water Management*, *65*(3), 193–

210. https://doi.org/10.1016/j.agwat.2003.09.002

Bierlen, R., Wailes, E. J., & Crammer, G. L. (1997). The Mercosur rice economy.

Arkansas Agricultural Experiment Station Bulletins, *954*, 1–58.

Biggs, T. W., Scott, C. A., Gaur, A., Venot, J. P., Chase, T., & Lee, E. (2008). Impacts of

irrigation and anthropogenic aerosols on the water balance, heat fluxes, and surface

temperature in a river basin. *Water Resources Research*, *44*(12).

https://doi.org/10.1029/2008WR006847

Board, J. E., Peterson, M. L., & Ng, E. (1980). Floret sterility in rice in a cool

environment. *Agronomy Journal*, *72*(3), 483–487.

Boucher, O., Myhre, G., & Myhre, A. (2004). Direct human influence of irrigation on

atmospheric water vapour and climate. *Climate Dynamics*, *22*(6–7), 597–603.

https://doi.org/10.1007/s00382-004-0402-4

Bouman, B. A. M., Humphreys, E., Tuong, T. P., & Barker, R. (2007). *Rice and Water*. *Advances in Agronomy* (Vol. 92). Elsevier Masson SAS. https://doi.org/10.1016/S0065-2113(04)92004-4

Bouman, B. A. M., Kropff, M. J., Tuong, T. P., Wopereis, M. C. S., Ten Berge, H. F. M., & van Laar, H. H. (2001). *ORYZA2000: Modeling lowland rice* (Vol. 1). IRRI.

Bouman, B. A. M., & Van Laar, H. H. (2006). Description and evaluation of the rice growth model ORYZA2000 under nitrogen-limited conditions. *Agricltural Systems*, *87*(3), 249–273. https://doi.org/10.1016/j.agsy.2004.09.011

Brazilian Institute for Geography and Statistics. (2015). Systematic Survey of Agricultural Production (in Portuguese). Retrieved January 18, 2016, from http://www.ibge.gov.br/home/estatistica/indicadores/agropecuaria/lspa/default_publ _completa.shtm

Brouwer, C., Prins, K., & Heibloem, M. (1989). *Irrigation water management: Irrigation scheduling*. *FAO Training manual* (Vol. 4). Retrieved from http://www.fao.org/docrep/t7202e/t7202e00.HTM

Bunce, J. A. (2013). Effects of pulses of elevated carbon dioxide concentration on stomatal conductance and photosynthesis in wheat and rice. *Physiologia Plantarum*, *149*(2), 214–221. https://doi.org/10.1111/ppl.12026

Campbell, G. S., & Norman, J. M. (1998). *An Introduction to Environmental Biophysics* (Second Edi). New York: Springer.

Castañeda, A. R., Bouman, B. A. M., Peng, S., & Visperas, R. M. (2002). The potential of aerobic rice to reduce water use in water-scarce irrigated lowlands in the tropics. In B. A. M. Bouman, H. Hengsdijk, B. Hardy, P. S. Bindraban, T. P. Tuong, & J. K.

Ladha (Eds.), *Water-wise rice production* (pp. 165–176). Los Baños, Philippines: International Rice Research Institute.

Chapagain, A. K., & Hoekstra, A. Y. (2011). The blue, green and grey water footprint of rice from production and consumption perspectives. *Ecological Economics*, *70*(4), 749–758. https://doi.org/10.1016/j.ecolecon.2010.11.012

Chowdhury, S. I., & Wardlaw, I. F. (1978). The effect of temperature on kernel development in cereals. *Australian Journal of Agricultural Research*, *29*(2), 205–223. https://doi.org/10.1071/AR9780205

Chung, S.-O., Rodríguez-Díaz, J. A., Weatherhead, E. K., & Knox, J. W. (2011). Climate change impacts on water for irrigating paddy rice in South Korea. *Irrigation and Drainage*, *60*(2), 263–273. https://doi.org/10.1002/ird.559

Collatz, G., Ribas-Carbo, M., & Berry, J. (1992). Coupled photosynthesis-stomatal conductance model for leaves of C_4 plants. *Australian Journal of Plant Physiology*, *19*(5), 519–538.

Counce, P. A., Keisling, T. C., & Mitchell, A. J. (2000). A uniform, objective, and adaptative system for expressing rice development. *Crop Science*, *40*(2), 436–443. https://doi.org/10.2135/cropsci2000.402436x

Cuadra, S. V., Costa, M. H., Kucharik, C. J., Da Rocha, H. R., Tatsch, J. D., Inman-Bamber, G., … Cabral, O. M. R. (2012). A biophysical model of Sugarcane growth. *Global Change Biology Bioenergy*, *4*(1), 36–48. https://doi.org/10.1111/j.1757-1707.2011.01105.x

De Silva, C. S., Weatherhead, E. K., Knox, J. W., & Rodriguez Díaz, J. A. (2007). Predicting the impacts of climate change - A case study of paddy irrigation water

requirements in Sri Lanka. *Agricultural Water Management*, *93*(1–2), 19–29.

https://doi.org/10.1016/j.agwat.2007.06.003

Delire, C., & Foley, J. A. (1999). Evaluating the performance of a land Surface /

ecosystem model with biophysical measurements from contrasting environments.

Journal of Geophysical Research, *104*(D14), 16895–16909.

https://doi.org/10.1029/1999JD900212

Deryng, D., Conway, D., Ramankutty, N., Price, J., & Warren, R. (2014). Global crop

yield response to extreme heat stress under multiple climate change futures.

Environmental Research Letters, *9*(3), 34011. https://doi.org/10.1088/1748-

9326/9/3/034011

Dingkuhn, M., Sow, A., Samb, A., Diack, S., & Asch, F. (1995). Climatic determinants

of irrigated rice performance in the Sahel - I. Photothermal and micro-climatic

responses of flowering. *Agricultural Systems*, *48*(4), 385–410.

https://doi.org/10.1016/0308-521X(94)00027-I

Döll, P. (2002). Impact of climate change and variability on irrigation requirements: A

global perspective. *Climatic Change*, *54*(3), 269–293.

https://doi.org/10.1023/A:1016124032231

El Maayar, M., Price, D. T., Black, T. A., Humphreys, E. R., & Jork, E. M. (2002).

Sensitivity tests of the integrated biosphere simulator to soil and vegetation

characteristics in a Pacific coastal coniferous forest. *Atmosphere-Ocean*, *40*(3), 313–

332. https://doi.org/10.3137/ao.400303

El Maayar, M., Price, D. T., Delire, C., Foley, J. A., Black, T. A., & Bessemoulin, P.

(2001). Validation of the Integrated Biosphere Simulator over Canadian deciduous

and coniferous boreal forest stands. *Journal of Geophysical Research-Atmospheres*, *106*(D13), 14339–14355. https://doi.org/10.1029/2001jd900155

Erda, L., Wei, X., Hui, J., Yinlong, X., Yue, L., Liping, B., & Liyong, X. (2005). Climate change impacts on crop yield and quality with CO2 fertilization in China. *Philosophical Transactions of the Royal Society B: Biological Sciences*, *360*(1463), 2149–2154. https://doi.org/10.1098/rstb.2005.1743

FAO. (2016). FAOSTAT database collections. Retrieved May 10, 2016, from http://faostat3.fao.org/home/E

Farquhar, G. D., Von Caemmerer, S., & Berry, J. A. (1980). A biochemical model of photosynthetic CO_2 assimilation in leaves of C_3 species. *Planta*, *149*, 78–90. https://doi.org/10.1007/BF00386231

Farrell, T. C., Fox, K. M., Williams, R. L., & Fukai, S. (2006). Genotypic variation for cold tolerance during reproductive development in rice: Screening with cold air and cold water. *Field Crops Research*, *98*(2–3), 178–194. https://doi.org/10.1016/j.fcr.2006.01.003

Foley, J. A., Prentice, I. C., Ramankutty, N., Levis, S., Pollard, D., Sitch, S., & Haxeltine, A. (1996). An integrated biosphere model of land surface processes. *Global Biogeochemical Cycles*, *14*(3), 795–825.

Georgescu, M., Lobell, D. B., & Field, C. B. (2011). Direct climate effects of perennial bioenergy crops in the United States. *Proceedings of the National Academy of Sciences of the United States of America*, *108*(11), 4307–12. https://doi.org/10.1073/pnas.1008779108

Giorgi, F., & Diffenbaugh, N. (2008). Developing regional climate change scenarios for

use in assessment of effects on human health and disease. *Climate Research*, *36*(2), 141–151. https://doi.org/10.3354/cr00728

Giorgi, F., Jones, C., & Asrar, G. R. (2009). Addressing climate information needs at the regional level: The CORDEX framework. *World Meteorological Organization Bulletin*, *58*(3), 175–183.

Gudmundsson, L., Bremnes, J. B., Haugen, J. E., & Engen Skaugen, T. (2012). Technical Note: Downscaling RCM precipitation to the station scale using quantile mapping – a comparison of methods. *Hydrology and Earth System Sciences Discussions*, *9*(5), 6185–6201. https://doi.org/10.5194/hessd-9-6185-2012

Harris, I., Jones, P. D., Osborn, T. J., & Lister, D. H. (2014). Updated high resolution grids of monthly climatic observations - the CRU TS3.10 Dataset. *International Journal of Climatology*, *34*(3), 623–642.

Hatfield, J. L., & Prueger, J. H. (2015). Temperature extremes: Effect on plant growth and development. *Weather and Climate Extremes*, *10*, 4–10. https://doi.org/10.1016/j.wace.2015.08.001

Horie, T. (1993). Predicting the effects of climatic variation and elevated CO2 on rice yield in Japan. *Journal of Agricultural Meteorology*, *48*(5), 567–574.

IPCC. (2013). *Climate Change 2013: The Physical Science Basis. Contribution of Working Group I to the Fifth Assessment Report of the Intergovernmental Panel on Climate Change*. *IPCC* (Vol. AR5). Cambridge, United Kingdom and New York, NY, USA: Cambridge University Press.

Jagadish, S. V. K., Craufurd, P. Q., & Wheeler, T. R. (2007). High temperature stress and spikelet fertility in rice (Oryza sativa L.). *Journal of Experimental Botany*, *58*(7),

1627–1635. https://doi.org/10.1093/jxb/erm003

Kaneda, C., & Beachell, H. M. (1974). Response of indica-japonica rice hybrids to low
temperatures. *SABRAO*, *6*, 17–32.

Khush, G. S. (2005). What it will take to Feed 5.0 Billion Rice consumers in 2030. *Plant
Molecular Biology*, *59*(1), 1–6. https://doi.org/10.1007/s11103-005-2159-5

Kim, H.-Y., Lieffering, M., Kobayashi, K., Okada, M., & Miura, S. (2003). Seasonal
changes in the effects of elevated CO2 on rice at three levels of nitrogen supply: a
free air CO2 enrichment (FACE) experiment. *Global Change Biology*, *9*(6), 826–
837. https://doi.org/10.1046/j.1365-2486.2003.00641.x

Kimball, B. A. (1983). Carbon Dioxide and Agricultural Yield: An Assemblage and
Analysis of 430 Prior Observations. *Agronomy Journal*, *75*(5), 779.
https://doi.org/10.2134/agronj1983.00021962007500050014x

Kimball, B. A. (2016). Crop responses to elevated CO2 and interactions with H2O, N,
and temperature. *Current Opinion in Plant Biology*, *31*, 36–43.
https://doi.org/10.1016/j.pbi.2016.03.006

Kimball, B. A., Kobayashi, K., & Bindi, M. (2002). Responses of agricultural crops to
free-air CO2 enrichment. In *Advances in Agronomy* (Vol. Volume 77, pp. 293–368).
https://doi.org/http://dx.doi.org/10.1016/S0065-2113(02)77017-X

Kiniry, J. R., Rosenthal, W. D., Jackson, B. S., & Hoogenboom, G. (1991). Predicting
leaf development of crop plants. In *Predicting Crop Phenology*. Boca Raton, FL:
CRC Press.

Klein, S. A., Zhang, Y., Zelinka, M. D., Pincus, R., Boyle, J., & Gleckler, P. J. (2013).
Are climate model simulations of clouds improving? An evaluation using the ISCCP

simulator. *Journal of Geophysical Research Atmospheres*, *118*(3), 1329–1342. https://doi.org/10.1002/jgrd.50141

Konzmann, M., Gerten, D., & Heinke, J. (2013). Climate impacts on global irrigation requirements under 19 GCMs, simulated with a vegetation and hydrology model. *Hydrological Sciences Journal*, *58*(1), 88–105. https://doi.org/10.1080/02626667.2013.746495

Kucharik, C. J. (2003). Evaluation of a Process-Based Agro-Ecosystem Model (Agro-IBIS) across the U.S. Corn Belt: Simulations of the Interannual Variability in Maize Yield. *Earth Interactions*, *7*(14), 1–33. https://doi.org/10.1175/1087-3562(2003)007<0001:EOAPAM>2.0.CO;2

Kucharik, C. J., & Brye, K. R. (2003). Integrated BIosphere Simulator (IBIS) yield and nitrate loss predictions for Wisconsin maize receiving varied amounts of nitrogen fertilizer. *Journal of Environment Quality*, *32*(1), 247–268. https://doi.org/10.2134/jeq2003.2470

Kucharik, C. J., Foley, J., Delire, C., Fisher, V. a., Coe, M. T., Lenters, J. D., … Gower, S. T. (2000). Testing the performance of a dynamic global ecosystem model: Water balance, carbon balance, and vegetation structure. *Global Biogeochemical Cycles*, *14*(3), 795–825. https://doi.org/10.1029/1999GB001138

Kucharik, C. J., & Twine, T. E. (2007). Residue, respiration, and residuals: Evaluation of a dynamic agroecosystem model using eddy flux measurements and biometric data. *Agricultural and Forest Meteorology*, *146*(3–4), 134–158. https://doi.org/10.1016/j.agrformet.2007.05.011

Kucharik, C. J., VanLoocke, A., Lenters, J. D., & Motew, M. M. (2013). Miscanthus

Establishment and Overwintering in the Midwest USA: A Regional Modeling Study of Crop Residue Management on Critical Minimum Soil Temperatures. *PLoS ONE*, *8*(7). https://doi.org/10.1371/journal.pone.0068847

Levis, S., Bonan, G. B., Kluzek, E., Thornton, P. E., Jones, A., Sacks, W. J., & Kucharik, C. J. (2012). Interactive Crop Management in the Community Earth System Model (CESM1): Seasonal Influences on Land–Atmosphere Fluxes. *Journal of Climate*, *25*(14), 4839–4859. https://doi.org/10.1175/JCLI-D-11-00446.1

Li, Y., Gao, Y., Xu, X., Shen, Q., & Guo, S. (2009). Light-saturated photosynthetic rate in high-nitrogen rice (Oryza sativa L.) leaves is related to chloroplastic CO_2 concentration. *Journal of Experimental Botany*, *60*(8), 2351–2360. https://doi.org/10.1093/jxb/erp127

Lin, W., Ziska, L. H., Namuco, O. S., & Bai, K. (1997). The interaction of high temperature and elevated CO_2 on photosynthetic acclimation of single leaves of rice in situ. *Physiologia Plantarum*, *99*(1), 178–184. https://doi.org/10.1111/j.1399-3054.1997.tb03446.x

Lu, W., Cheng, W., Zhang, Z., Xin, X., & Wang, X. (2015). Differences in rice water consumption and yield under four irrigation schedules in central Jilin Province, China. *Paddy and Water Environment*. https://doi.org/10.1007/s10333-015-0516-9

Makino, A., Harada, M., Kaneko, K., Mae, T., Shimada, T., & Yamamoto, N. (2000). Whole-plant growth and N allocation in transgenic rice plants with decreased content of ribulose-1,5-bisphosphate carboxylase under different CO_2 partial pressures. *Australian Journal of Plant Physiology*, *27*(1), 1–12. https://doi.org/10.1071/PP99094

Makino, A., Nakano, H., & Mae, T. (1994). Effects of Growth Temperature on the Responses of Ribulose-1,5-Biphosphate Carboxylase, Electron Transport Components, and Sucrose Synthesis Enzymes to Leaf Nitrogen in Rice, and Their Relationships to Photosynthesis. *Plant Physiology*, *105*(4), 1231–1238. https://doi.org/10.1104/pp.105.4.1231

Maraun, D., Wetterhall, F., Ireson, A. M., Chandler, R. E., Kendon, E. J., Widmann, M., … Thiele-Eich, I. (2010). Precipitation downscaling under climate change: Recent developments to bridge the gap between dynamical models and the end user. *Reviews of Geophysics*, *48*(3). https://doi.org/10.1029/2009RG000314

Marengo, J. A., Ambrizzi, T., da Rocha, R. P., Alves, L. M., Cuadra, S. V., Valverde, M. C., … Ferraz, S. E. T. (2010). Future change of climate in South America in the late twenty-first century: Intercomparison of scenarios from three regional climate models. *Climate Dynamics*, *35*(6), 1089–1113. https://doi.org/10.1007/s00382-009-0721-6

Marengo, J. A., Chou, S. C., Kay, G., Alves, L. M., Pesquero, J. F., Soares, W. R., … Tavares, P. (2012). Development of regional future climate change scenarios in South America using the Eta CPTEC/HadCM3 climate change projections: Climatology and regional analyses for the Amazon, S??o Francisco and the Paran?? River basins. *Climate Dynamics*, *38*(9–10), 1829–1848. https://doi.org/10.1007/s00382-011-1155-5

Maruyama, A., & Kuwagata, T. (2010). Coupling land surface and crop growth models to estimate the effects of changes in the growing season on energy balance and water use of rice paddies. *Agricultural and Forest Meteorology*, *150*(7–8), 919–930.

Matsui, T., Omasa, K., & Horie, T. (1997). High Temperature-Induced Spikelet Sterility of Japonica Rice at Flowering in Relation to Air Temperature, Humidity and Wind Velocity Conditions. *Japanese Journal of Crop Science*, *66*, 449–455. https://doi.org/10.1626/jcs.66.449

McLean, J., Hardy, B., & Hettel, G. (2013). *Rice Almanac, 4th edition. IRRI, Los Baños, Philippines*. https://doi.org/10.1093/aob/mcg189

Monfreda, C., Ramankutty, N., & Foley, J. A. (2008). Farming the planet: 2. Geographic distribution of crop areas, yields, physiological types, and net primary production in the year 2000. *Global Biogeochemical Cycles*, *22*(1). https://doi.org/10.1029/2007GB002947

Nagai, T., & Makino, A. (2009). Differences between rice and wheat in temperature responses of photosynthesis and plant growth. *Plant and Cell Physiology*, *50*(4), 744–755. https://doi.org/10.1093/pcp/pcp029

Nakagawa, H., Horie, T., Kim, H. Y., Ohnishi, H., & Homma, K. (1997). Rice Responses to Elevated CO2 Concentrations and High Temperatures. *Journal of Agricultural Meteorology*, *52*(5), 797–800.

National Supply Company. (2016). *Agricultural production costs (in portuguese)*. Retrieved from http://www.conab.gov.br/conteudos.php?a=1546&t=2

Nishiyama, I. (1984). Climatic influence on pollen formation and fertilization. In *Biology of rice* (Vol. 153, p. 171). Elsevier Amsterdam.

Nuñez, M. N., Solman, S. A., & Cabré, M. F. (2009). Regional climate change experiments over southern South America. II: Climate change scenarios in the late twenty-first century. *Climate Dynamics*, *32*(7–8), 1081–1095.

https://doi.org/10.1007/s00382-008-0449-8

Osborne, T., Gornall, J., Hooker, J., Williams, K., Wiltshire, A., Betts, R., & Wheeler, T. (2015). JULES-crop: A parametrisation of crops in the Joint UK Land Environment Simulator. *Geoscientific Model Development*, *8*(4), 1139–1155. https://doi.org/10.5194/gmd-8-1139-2015

Penning de Vries, F. W. T., Jansen, D. M., ten Berge, H. F. M., & Bakema, A. (1989). *Simulation of ecophysiological processes of growth in several annual crops*. Wageningen: Pudoc Wageningen.

Pollard, D., & Thompson, S. L. (1995). Use of a land-surface transfer scheme (LSX) in a global climate model: the response to doubling stomatal conductance. *Global Planetary Change*, *10*(1), 129–161.

Prasad, P. V. V, Boote, K. J., Allen, L. H., Sheehy, J. E., & Thomas, J. M. G. (2006). Species, ecotype and cultivar differences in spikelet fertility and harvest index of rice in response to high temperature stress. *Field Crops Research*, *95*(2–3), 398-411. https://doi.org/10.1016/j.fcr.2005.04.008

Ramankutty, N., Evan, A. T., Monfreda, C., & Foley, J. A. (2008). Farming the planet: 1. Geographic distribution of global agricultural lands in the year 2000. *Global Biogeochemical Cycles*, *22*(1). https://doi.org/10.1029/2007GB002952

Rawls, W. J., Ahuja, L. R., & Brakensiek, D. L. (1992). Estimating soil hydraulic properties from soil data. In M. T. van Genuchten, F. J. Leij, & L. J. Lund (Eds.), *Proc. Int. Workshop on Indirect Methods for Estimating the Hydraulic Properties of Unsatures Soils* (pp. 329–340). University of California, Riverside.

Richardson, C. W., & Wright, D. A. (1984). WGEN : A Model for Generating Daily

Weather Variables. *U. S. Department of Agriculture, Agricultural Research Service, ARS-8*, 83. Retrieved from http://soilphysics.okstate.edu/software/cmls/WGEN.pdf

Rodríguez Díaz, J. A., Weatherhead, E. K., Knox, J. W., & Camacho, E. (2007). Climate change impacts on irrigation water requirements in the Guadalquivir river basin in Spain. *Regional Environmental Change*, *7*(3), 149–159. https://doi.org/10.1007/s10113-007-0035-3

Roel, A., Mutters, R. G., Eckert, J. W., & Plant, R. E. (2005). Effect of low water temperature on rice yield in California. *Agronomy Journal*, *97*(3), 943–948. https://doi.org/10.2134/agronj2004.0129

Rosenzweig, C., Tubiello, F. N., Goldberg, R., Mills, E., & Bloomfield, J. (2002). Increased crop damage in the US from excess precipitation under climate change. *Global Environmental Change*. https://doi.org/10.1016/S0959-3780(02)00008-0

Rowland-Bamford, A. J., Baker, J. T., Allen, L. H., & Bowes, G. (1991). Acclimation of rice to changing atmospheric carbon dioxide concentration. *Plant, Cell & Environment*, *14*(6), 577–583. https://doi.org/10.1111/j.1365-3040.1991.tb01528.x

Ruiz-Vera, U. M., Siebers, M., Gray, S. B., Drag, D. W., Rosenthal, D. M., Kimball, B. A., … Bernacchi, C. J. (2013). Global warming can negate the expected CO_2 stimulation in photosynthesis and productivity for soybean grown in the Midwestern United States. *Plant Physiology*, *162*(1), 410–423. https://doi.org/Doi 10.1104/Pp.112.211938

Sánchez, B., Rasmussen, A., & Porter, J. R. (2014). Temperatures and the growth and development of maize and rice: A review. *Global Change Biology*, *20*(2), 408–417. https://doi.org/10.1111/gcb.12389

Seager, R., Ting, M., Li, C., Naik, N., Cook, B., Nakamura, J., & Liu, H. (2013).

Projections of declining surface-water availability for the southwestern United

States. *Nature Climate Change*, *3*(5), 482–486. https://doi.org/10.1038/nclimate1787

Shahid, S. (2011). Impact of climate change on irrigation water demand of dry season

Boro rice in northwest Bangladesh. *Climatic Change*, *105*(3–4), 433–453.

https://doi.org/10.1007/s10584-010-9895-5

South-Brazilian Society for Irrigated Rice. (2014). *Irrigated rice: technical research*

recommendations to southern Brazil (in portuguese). Retrieved from

http://www.irga.rs.gov.br/upload/20141205095320recomendacoes_tecnicas_sosbai_

2014.pdf

Soylu, M. E., Istanbulluoglu, E., Lenters, J. D., & Wang, T. (2011). Quantifying the

impact of groundwater depth on evapotranspiration in a semi-arid grassland region.

Hydrology and Earth System Sciences, *15*(3), 787–806. https://doi.org/10.5194/hess-

15-787-2011

Streck, N. A., Michelon, S., Bosco, L., Lago, I., Walter, L. C., Rosa, H. T., & Paula, G.

M. de. (2007). Thermal time of some developmental phases of the COUNCE scale

for irrigated rice cultivars grown in Southern Brazil. *Bragantia*, *66*, 357–364 [In

Portuguese]. Retrieved from

http://www.scielo.br/scielo.php?script=sci_arttext&pid=S0006-

87052007000200020&nrm=iso

Tao, F., Yokozawa, M., Xu, Y., Hayashi, Y., & Zhang, Z. (2006). Climate changes and

trends in phenology and yields of field crops in China, 1981-2000. *Agricultural and*

Forest Meteorology, *138*(1–4), 82–92. https://doi.org/10.1159/000092636

Taylor, K. E., Stouffer, R. J., & Meehl, G. A. (2012). An overview of CMIP5 and the experiment design. *Bulletin of the American Meteorological Society*. https://doi.org/10.1175/BAMS-D-11-00094.1

Timm, A. U., Roberti, D. R., Streck, N. A., de Gonçalves, L. G. G., Acevedo, O. C., Moraes, O. L. L., … Toll, D. L. (2014). Energy partitioning and evapotranspiration over a rice paddy in Southern Brazil. *Journal of Hydrometeorology*, *15*(5), 1975–1988. https://doi.org/10.1175/JHM-D-13-0156.1

Tsvetsinskaya, E. A., Mearns, L. O., & Easterling, W. E. (2001). Investigating the effect of seasonal plant growth and development in three-dimensional atmospheric simulations. Part II: Atmospheric response to crop growth and development. *Journal of Climate*, *14*(5), 711–729. https://doi.org/10.1175/1520-0442(2001)014<0711:ITEOSP>2.0.CO;2

Tuong, T. P., Cabangon, R. J., & Wopereis, M. C. S. (1996). Quantifying flow processes during land soaking of cracked rice soils. *Soil Science Society of America Journal*, *60*(3), 872–879.

Twine, T. E., Bryant, J. J., T. Richter, K., Bernacchi, C. J., Mcconnaughay, K. D., Morris, S. J., & Leakey, A. D. B. (2013). Impacts of elevated CO2 concentration on the productivity and surface energy budget of the soybean and maize agroecosystem in the Midwest USA. *Global Change Biology*, *19*(9), 2838–2852. https://doi.org/10.1111/gcb.12270

Usui, Y., Sakai, H., Tokida, T., Nakamura, H., Nakagawa, H., & Hasegawa, T. (2016). Rice grain yield and quality responses to free-air CO2 enrichment combined with soil and water warming. *Global Change Biology*, *22*(3), 1256–1270.

https://doi.org/10.1111/gcb.13128

van Vuuren, D. P., Edmonds, J., Kainuma, M., Riahi, K., Thomson, A., Hibbard, K., …
Rose, S. K. (2011). The representative concentration pathways: An overview.
Climatic Change, *109*(1), 5–31. https://doi.org/10.1007/s10584-011-0148-z

Vanloocke, A., Bernacchi, C. J., & Twine, T. E. (2010). The impacts of Miscanthus x
giganteus production on the Midwest US hydrologic cycle. *Global Change Biology
Bioenergy*, *2*(4), 180–191. https://doi.org/DOI 10.1111/j.1757-1707.2010.01053.x

Vergara, B., & Chang, T. (1985). *The flowering response of rice to photoperiod: A
review of the literature*. *International Rice Research Institute (IRRI)*. Retrieved from
http://books.google.com/books?hl=en&lr=&id=TCtF5INb-
f0C&oi=fnd&pg=PP2&dq=The+flowering+response+of+the+rice+plant+to+photop
eriod,+a+review+of+the+literature&ots=xEPmkEXa37&sig=4e3dZ2p1D3hdi9c18q
RZCZKB_lg

Vu, J. C. V, Allen Jr., L. H., & Bowes, G. (1997). Effects of elevated CO2 and
temperature on photosynthesis and Rubisco in rice and soybean. *Plant Cell and
Environment*, *20*(1), 68–76. https://doi.org/10.1046/j.1365-3040.1997.d01-10.x

Yoshida, S. (1981). *Fundamentals of Rice Crop Science*. *Fundamentals of rice crop
science*. Retrieved from http://hdl.handle.net/10269/223

Zhang, T., Huang, Y., & Yang, X. (2013). Climate warming over the past three decades
has shortened rice growth duration in China and cultivar shifts have further
accelerated the process for late rice. *Global Change Biology*, *19*(2), 563–570.
https://doi.org/10.1111/gcb.12057

Ziska, L. H., Weerakoon, W., Namuco, O. S., & Pamplona, R. (1996). The influence of

nitrogen on the elevated CO2 response in field-grown rice. *Australian Journal of*

Plant Physiology, *23*(1), 45–52 LA–English. https://doi.org/10.1071/PP9960045

Zullo, J., Pinto, H. S., Assad, E. D., & Ávila, A. M. H. (2011). Potential for growing

Arabica coffee in the extreme south of Brazil in a warmer world. *Climatic Change*,

109(3–4), 535–548. https://doi.org/10.1007/s10584-011-0058-0

Appendix A

In this section I evaluate the performance of the CMIP5 models used in our

simulations by comparing their raw and corrected historical output for precipitation,

temperature, cloudiness and humidity against CRU observations.

<u>Precipitation</u>

Figure 23 shows quantile-quantile plots (Q-Q plots) between every CMIP5 model

against CRU observations, before and after bias correction. The closer the data points are

to the 1:1 line, the more similar the data distribution of the models is to the observed data

distribution. If data points are above the line, then the simulated data distribution is

skewed to the right compared to the observed data distribution (which can be interpreted

as an overestimation trend), and vice versa.

For southern Brazil, CanESM2 overestimates rainfall greater than 10 mm month^{-1}.

GFDL-ESM2 underestimates rainfall by between 1 mm month^{-1} and 8 mm month^{-1} and

slightly overestimates rainfall by between 12 mm month^{-1} and 15 mm month^{-1}. MRI-

CGCM3 and NorESM1-M slightly underestimates rainfall lower than 7 mm month^{-1} and

between 14 mm month^{-1} and 18 mm month^{-1}. INMCM4 consistently underestimates

rainfall. After bias correction, in general all models except GFDL's ESM2M had excessive heavy (greater than 15 mm day^{-1}) rainfall events compared to observations. This effect is well known because the quantile mapping model does not take into account the tails of the data distribution (Maraun et al., 2010). Analyzing the frequency and temporal occurrence of these events or their impact on the irrigation model is beyond the scope of this work.
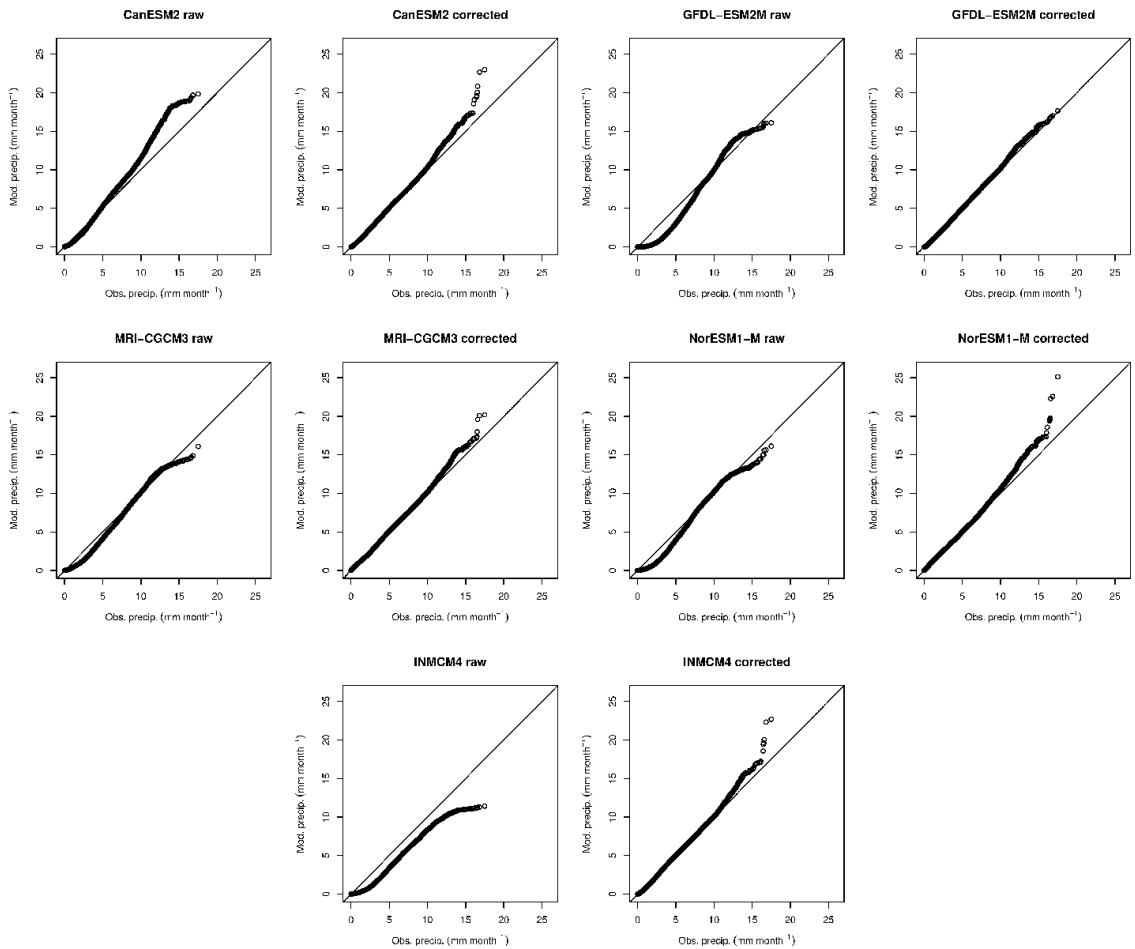

Figure 23. Quantile-quantile plots of simulated rainfall by CMIP5 models CanESM2, GFDL-ESM2M, MRI-CGCM3, NorESM1 and INMCM4 against CRU observations. For each pair of plots, raw (left) and corrected (right) model output were compared against observations. Data points shown in each plot correspond to monthly values of all 437 grid cells in southern Brazil, encompassing the 15-year period from 1996 to 2010 (sample size is 78660 points).

Figure 24 shows the spatial distribution of the seasonal mean precipitation (mm month^{-1}) as in CRU and as simulated by the selected CMIP5 models after bias correction. During the DJF period, MRI-CGCM3 exhibits a good representation of the precipitation pattern over southern Brazil, but CanESM2, GFDL-ESM2M, NorESM1-M and INM-CM4 are wetter then observations.

In the MAM and JJA periods, although general patterns are similar to CRU, CMIP5 models show some divergences. All models but MRI-CGCM3 underestimates precipitation in MAM and it is the only model that does not underestimate precipitation in JJA. In SON, months where rice is typically sown in southern Brazil, all the models but GFDL-ESM2M overestimate precipitation in southern Brazil.
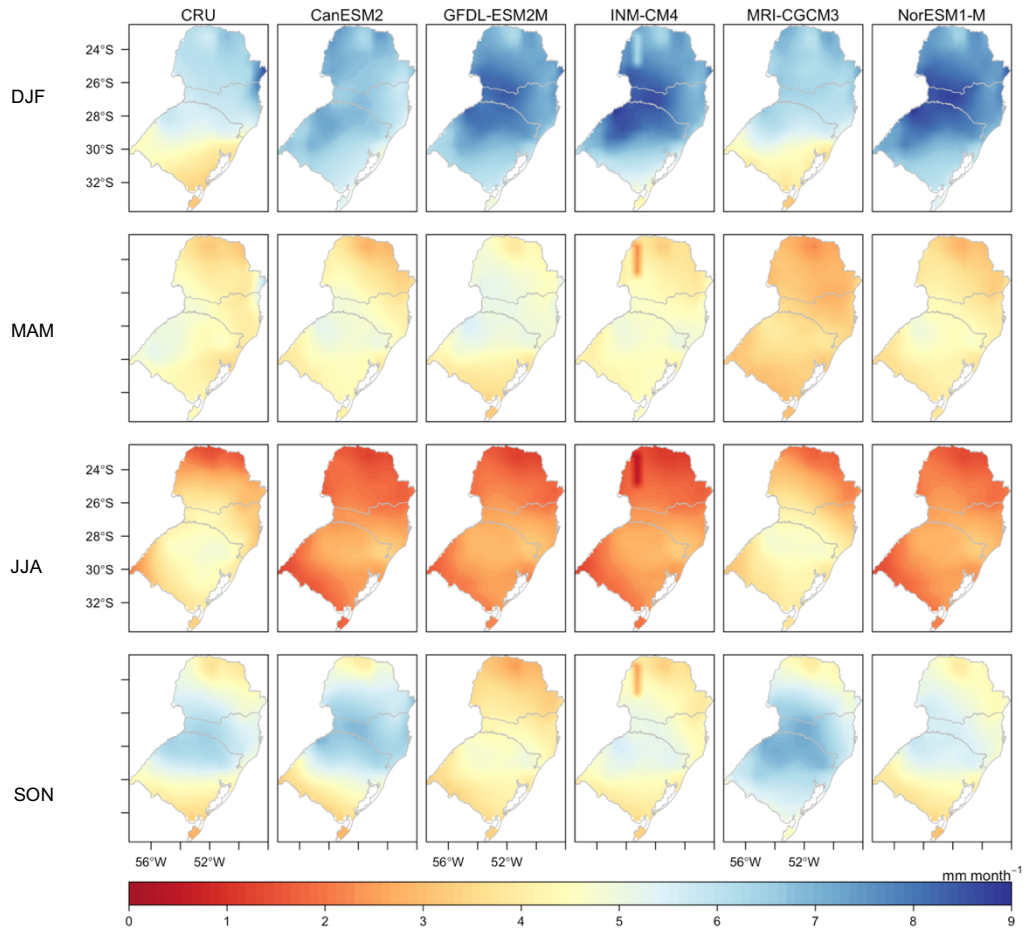
Figure 24. Seasonal daily mean precipitation (mm month^{-1}) for the period 1981-2010 as in CRU and simulated by CanESM2, GFDL-ESM2M, INM-CM4, MRI-CGCM3 and NorESM1 (depicted in the columns), during the months December to February (DJF), March to May (MAM), June to August (JJA) and September to November (SON), depicted in the rows.

Temperature

In general temperature was the climatic variable where the raw models output compared the best to the observations. As seen in Figure 25, all models except NorESM1-M (and especially GFDL-ESM2M) have a warm bias (particularly in

temperatures higher than 25°C). On the other hand, INM-CM4 tends to underestimate temperatures below 25°C.
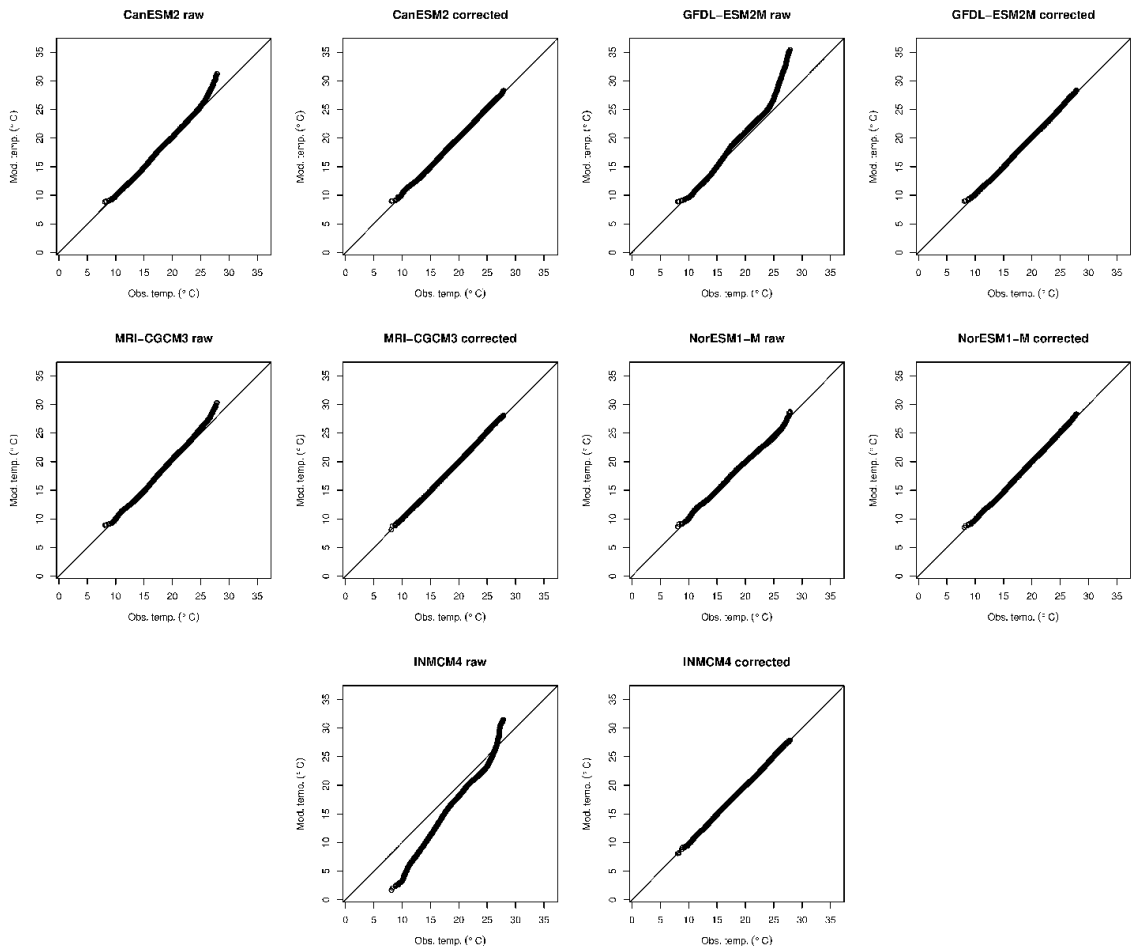

Figure 25. As in Figure 23, but for temperature (°C).

The spatial distribution of the seasonal mean temperature (°C), depicted in Figure 26, shows that most of the systematic biases suggested in Figure 25 were removed by the quantile mapping procedure. The only notable exception is during SON where GFDL-ESM2M is slightly hotter than observations in the northern and western portions of the study area.
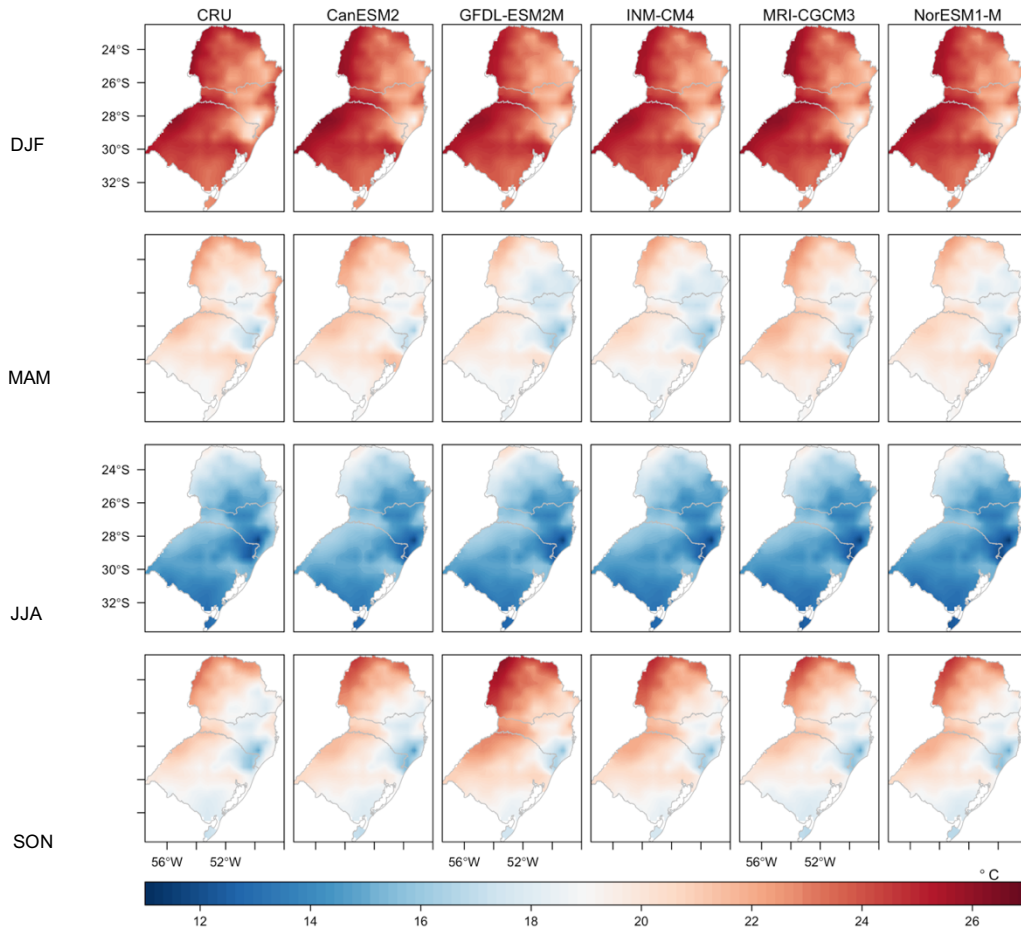
Figure 26. As in Figure 24, but for temperature (°C).

Cloudiness

It is well known that general circulation models (GCMs) tend to underestimate cloudiness (e.g. Klein et al. 2013), and our results support those findings (Figure 27). After performing bias correction, the models still exhibit underestimation of cloudiness in values close to 100%.
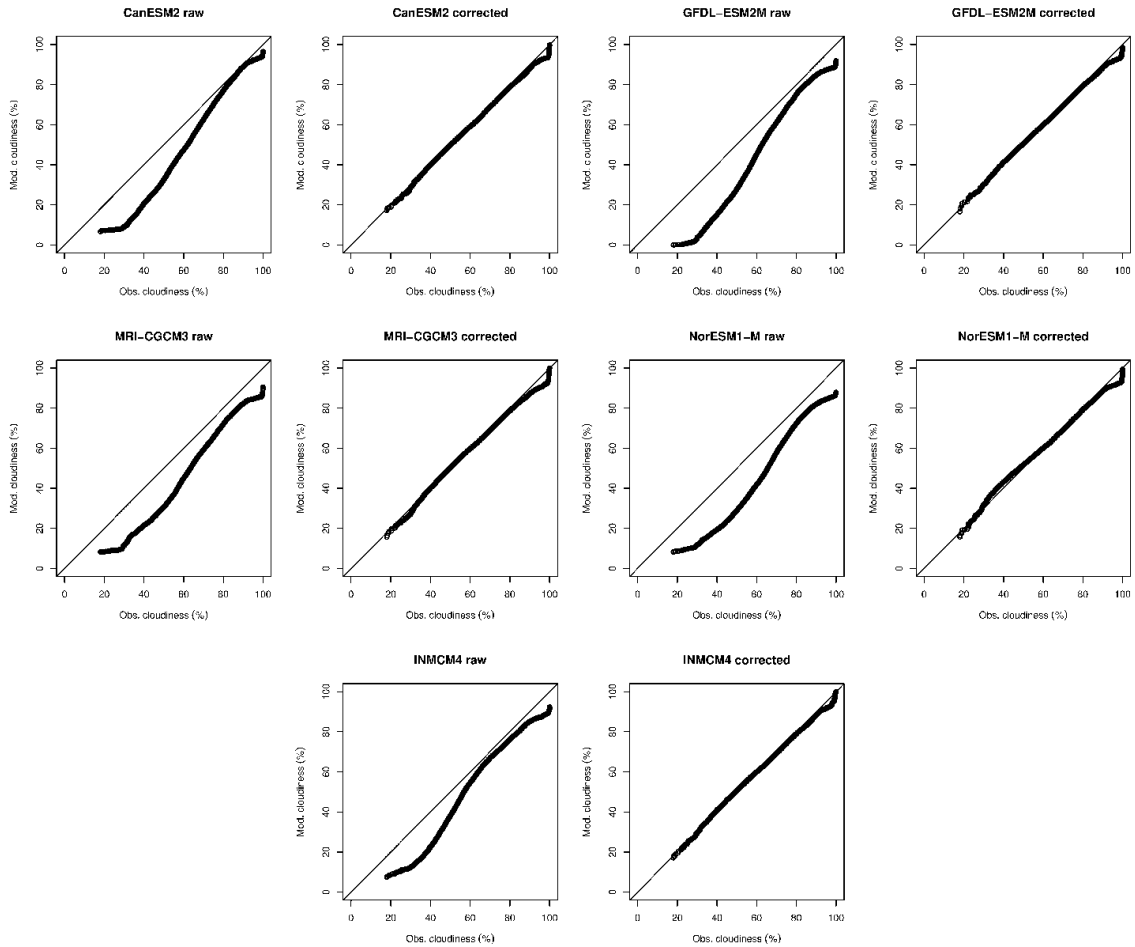
Figure 27. As in Figure 23, but for cloudiness.

Seasonal maps of cloudiness (%) from CMIP5 versus reference data sets (Figure 28) show a good concordance in austral summer (DJF) and spring (SON). During austral fall (MAM), MRI-CGCM-3 tends to underestimate cloudiness in western PR, SC and RS, and in the winter (JJA) all models except MRI-CGCM-3 have a lower cloud cover than observations in western PR, SC and RS.
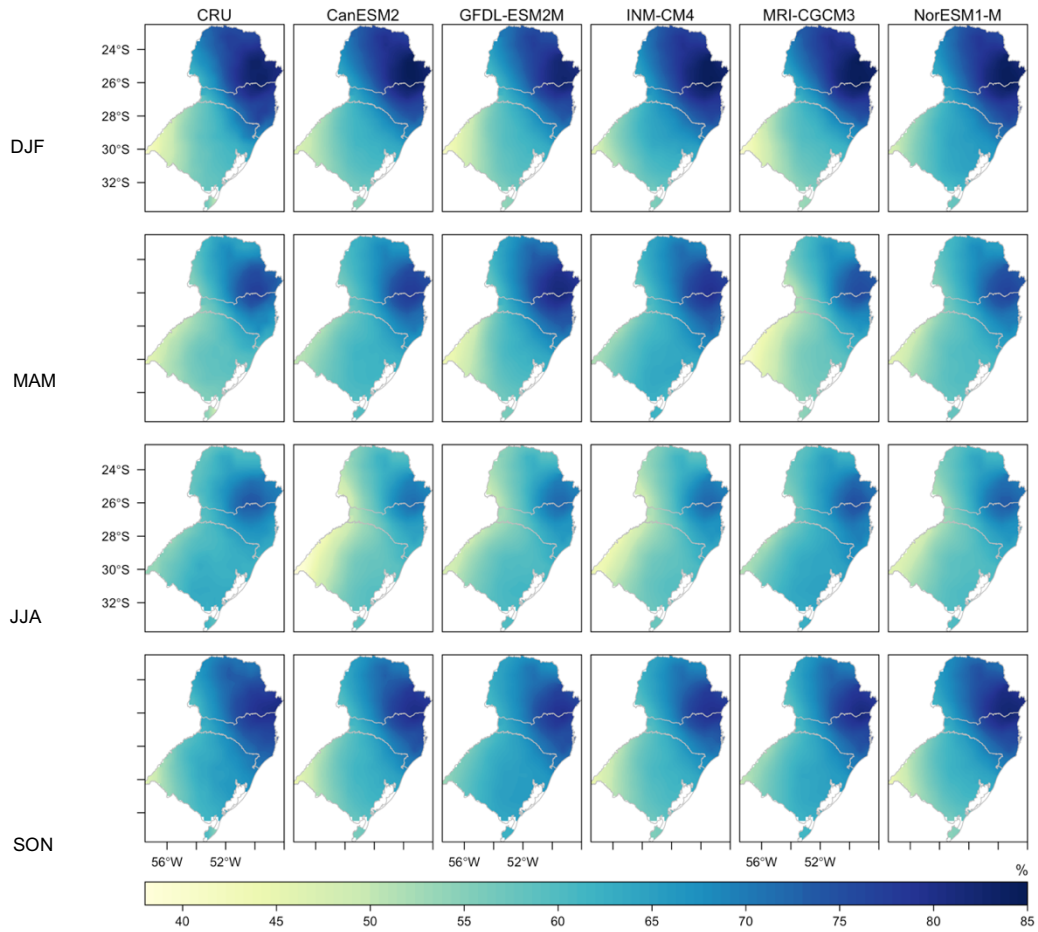
Figure 28. As in Figure 24, but for cloudiness (%).

Relative humidity

Figure 29 shows that, except for the CanESM2 model, there is a common model bias of underestimating relative humidity over southern Brazil.
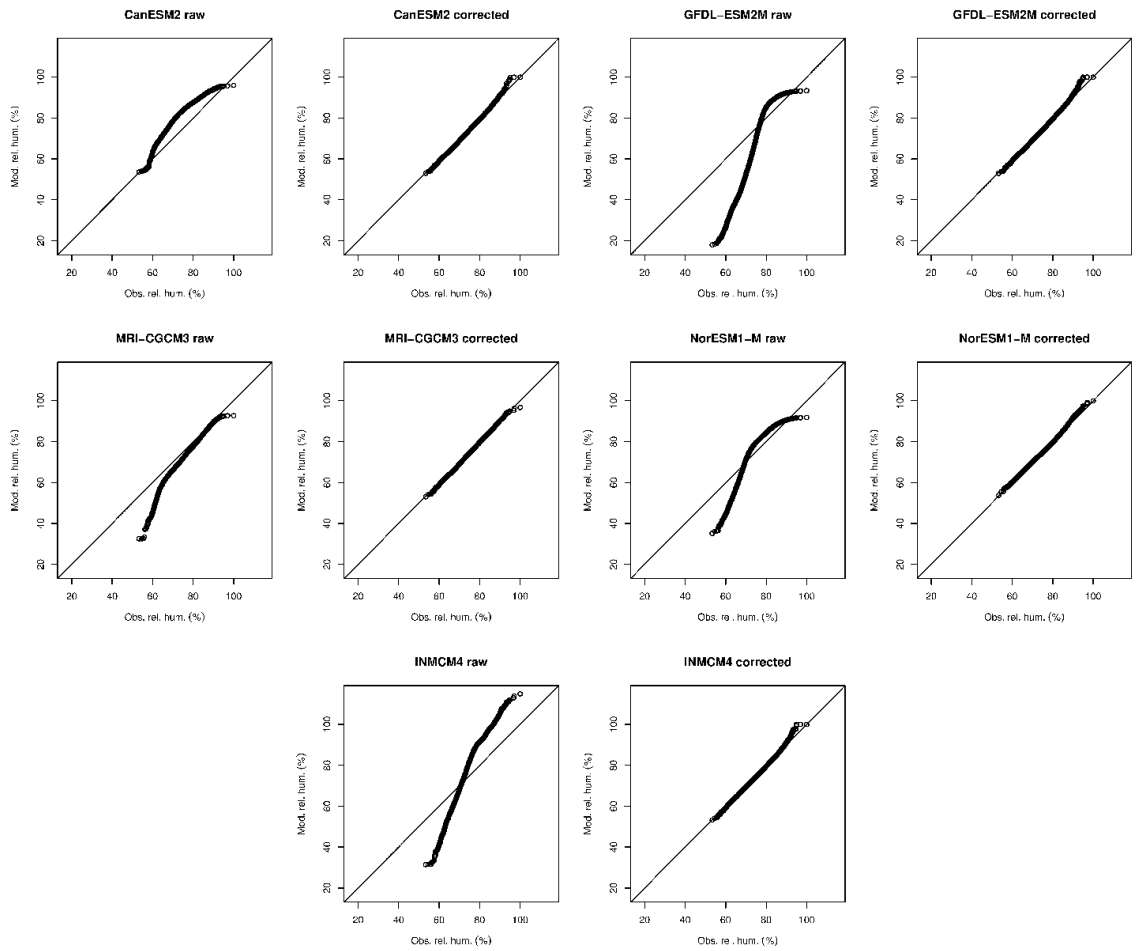
Figure 29. As in Figure 23, but for relative humidity.

In terms of the spatial pattern (Figure 30), the corrected output of the models was able to capture the interseasonal variability of observed relative humidity.
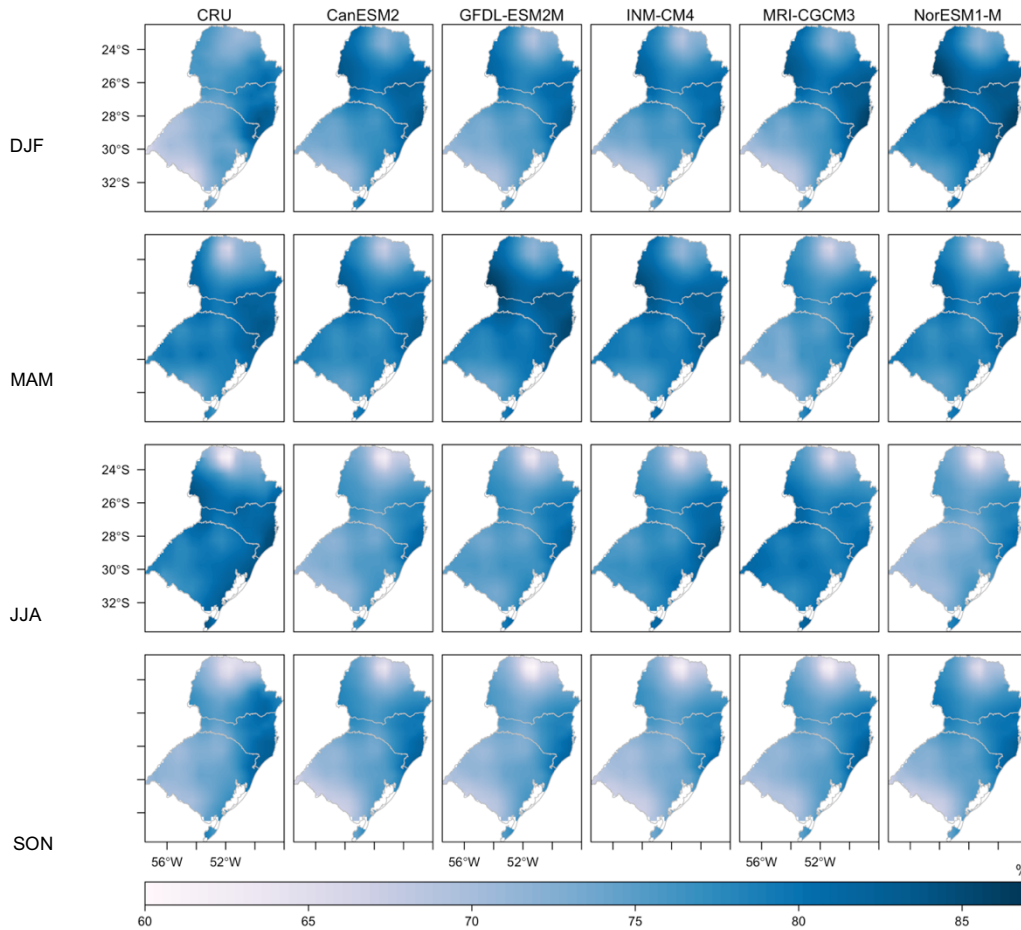
Figure 30. As in Figure 24, but for relative humidity (%).

Based on the results of this section, it is reasonable to state that none of the five models analyzed in this work performs well for all variables without any kind of bias correction. Overall, the quantile mapping bias correction method was generally capable of reducing errors in model outputs and producing more realistic seasonal cycles of precipitation, temperature, cloudiness and relative humidity. This assessment also shows that the individual CMIP5 models have large variability representing the historical climate system in southern Brazil, and highlights the importance of using multi-model ensemble mean as a way to reduce model biases.

Appendix B

This appendix provides the parameters for rice growth and irrigation used in the present study. Along with the development rates shown in Table 3, these are the parameters that need to be calibrated in order for Agro-IBIS realistically simulate rice growth at the calibration site.

Table 13. Rice crop growth parameters used in the Agro-IBIS model

Parameter	Value	Reference
Crop growth constants		
Base temperature for development (°C)	11	Bouman et al. (2001);
Maximum temperature for development (°C)	40	Streck et al. (2007)
Number of days between maturity and harvest	10	Present study
Canopy constants		
Maximum Rubisco activity at 15°C (μmol CO_2 m^{-2} s^{-1})	41	Li et al. (2009)
Specific leaf area (m^2 kg^{-1})	14	Asch et al. (1999)
Leaf orientation factor (-1 vertical, 0 random, 1 horizontal)	-0.5	Model's default
Low temperature threshold in tempvm equation (°C)	9	Bouman et al. (2001)
High temperature threshold in tempvm equation (°C)	38	
Carbon allocation		
Initial value of allocation fraction to fine roots	0.5	Present study
Final value of allocation fraction to fine roots	0.1	Present study
Irrigation constants		
Initial ponded water depth (mm)	70	South-Brazilian Society for Irrigated Rice, 2014
Minimum ponded water depth (mm)	30	
Maximum depth of ponded water (mm)	100	

Most of the crop parameters for rice are generic and can be used for all varieties (e.g. carbon allocation). However, some parameters are best calibrated specifically for the studied variety and environment. Development rate (DVR_c) of the crop is calculated based on the daily increment in heat units for the four different phenological stages

(section 3.3). Observations of phenology (dates of sowing, panicle initiation, flowering and physiological maturity) should be made in order to identify the duration of each growth phase. Hourly mean air temperature needs to be retrieved either from a local weather station or downscaled from a climate dataset to calculate the temperature sums for each growing stage using Eq. (1) and Eq. (2). The development rate for each growth phase (DVR_{phase}) can now be derived as the quotient between the DVS range and the temperature sum correspondent of each growth phase. The temporal progression of phenological indicator DVS is an integration of the crop development rate DVR_c over the growing season.

Any dry matter produced by the crop is partitioned between shoots and roots according to partitioning coefficients defined as a function of the phenological development stage, as shown by Eq. (9) through Eq. (11). Hence, a realistic calibration of the development rate for each growth phase is required to realistically represent the plant's phenological indicator DVS that is used to distribute the assimilated dry matter to leaves, stems, and reproductive organs. This is essentially the same approach as Agro-IBIS, except that the original phenological age indicator and allocation rules have been replaced by Oryza2000's. Parameters for rice physiology can be retrieved from literature when there are no measurements available, and then fine-tuned by model fitting (refining the parameter value until simulated variables under consideration best agreed with measured variables).